

Testing the Wineland Criterion with Finite Statistics

E. S. Carrera,^{*} Y. Zhang,^{*} J-D. Bancal, and N. Sangouard

Université Paris-Saclay, CEA, CNRS, Institut de physique théorique, 91191, Gif-sur-Yvette, France

(Dated: May 6, 2025)

The Wineland parameter aims at detecting metrologically useful entangled states, called spin-squeezed states, from expectations and variances of total angular momenta. However, efficient strategies for estimating this parameter in practice have yet to be determined and in particular, the effects of a finite number of measurements remain insufficiently addressed. We formulate the detection of spin squeezing as a hypothesis-testing problem, where the null hypothesis assumes that the experimental data can be explained by non-spin-squeezed states. Within this framework, we derive upper and lower bounds on the p-value to quantify the statistical evidence against the null hypothesis. By applying our statistical test to data obtained in multiple experiments, we are unable to reject the hypothesis that non-spin squeezed states were measured with a p-value of 5% or less in most cases. We also find an explicit non-spin squeezed state according to the Wineland parameter reproducing most of the observed results with a p-value exceeding 5%. More generally, our results provide a rigorous method to establish robust statistical evidence of spin squeezing from the Wineland parameter in future experiments, accounting for finite statistics.

Introduction — Quantum metrology leverages quantum mechanical effects to surpass the limitations of classical measurement techniques [1, 2], notably the standard quantum limit. Among the quantum states that can be utilized to enhance measurement precision [3–10], spin-squeezed states are receiving significant attention [11–22]. The condition for spin-squeezing is usually expressed in terms of the first and second moments of the angular momentum operator which is defined for N distinguishable $1/2$ spins as

$$J_\alpha = \frac{1}{2} \sum_{i=1}^N \sigma_\alpha^{(i)} \quad (1)$$

where $\alpha = x, y, z$ specifies the direction and $\sigma_\alpha^{(i)}$ is the corresponding Pauli matrix for spin i . More precisely, a state that fulfills [23]

$$\xi_W^2 = \frac{N \operatorname{Var}(J_{\vec{n}_\perp})}{\langle J_{\vec{n}} \rangle^2} < 1 \quad (2)$$

is said to be (metrologically) spin-squeezed along the \vec{n}_\perp direction. Here, $\langle J_{\vec{n}} \rangle$ denotes the expectation value of the spin operator along the direction \vec{n} and $\operatorname{Var}(J_{\vec{n}_\perp})$ is the variance of the spin in a direction \vec{n}_\perp orthogonal to \vec{n} . ξ_W^2 is called the Wineland parameter. Put simply, $\xi_W^2 < 1$ witnesses a class of quantum states where the collective spin variance is reduced in one direction while being increased in the orthogonal direction [23, 24]. In a Ramsey experiment, ξ_W^2 is established as the ratio of phase sensitivity of the state of interest $\hat{\rho}$ compared to a coherent spin state. Hence $\xi_W^2 < 1$ witnesses states having the potential to beat the standard quantum limit. The advantage of spin-squeezed states in metrology is due to quantum correlations between spins [24]. Specifically $\xi_W^2 < 1$ witnesses entanglement [25]. The ability to observe multiple spin states that are both metrologically useful and entangled through collective spin mea-

surements has driven numerous experimental implementations involving up to almost a million spins [11–22].

Experimentally confirming spin-squeezing has traditionally relied on the error bar associated to the estimation of the Wineland parameter. However, to demonstrate evidence of spin-squeezing, one should quantify the probability that the observed statistics, obtained from a limited number of experimental repetitions, could result from measurements on a state with no spin-squeezing, i.e. a state satisfying $\xi_W^2 \geq 1$. Error bars only quantify the spread of the measurement outcomes. They do not provide information about the likelihood that the observed data could have been produced by non-spin-squeezed states [26]. A more comprehensive statistical framework is thus needed for testing the Wineland criterion in practice. This challenge was highlighted in Refs. [27], where a similar issue emerged in the context of Bell correlation witnesses in many-spin systems.

In this letter, we develop a rigorous statistical framework for establishing robust evidence of spin squeezing based on the Wineland parameter, explicitly accounting for finite-size effects. Our approach focuses on quantifying the probability (p-value) that the observed experimental data could arise from a non-spin-squeezed state, thereby formulating the problem as a hypothesis test. Unlike the approach in Ref. [28], our analysis does not test a specific non-spin-squeezed state and enables the rejection of the hypothesis that *any* non-spin squeezed states could have produced the observed statistics with a specified p-value. Our findings indicate that most existing experiments do not sufficiently account for finite-size effects, with only a limited number of cases capable of rejecting the hypothesis test. In many situations, an insufficient number of measurements has been performed which result in a high probability that a non-spin-squeezed state could mimic the experimental outcomes, particularly when the total spin number is large.

Traditional approach — The verification of spin squeezing in experiments is typically based on the statistical estimation of the Wineland parameter ξ_W^2 . Conventional approaches involve measuring the total spin $\langle J_{\vec{n}} \rangle$ and the variance $\text{Var}(J_{\vec{n}\perp})$, followed by an evaluation of the uncertainty in ξ_W^2 from its error bar. A state is conventionally classified as spin-squeezed if the estimated value of ξ_W^2 falls below 1 with a sufficiently small error bar. However, error bars do not constitute a rigorous test for statistical significance [26]. In particular, they fail to account for the probability that statistical fluctuations may cause non-spin-squeezed states to satisfy $\xi_W^2 < 1$, leading to potential misclassification. To illustrate this risk, we conduct a Monte Carlo simulation by repeatedly measuring a non-spin-squeezed state of 9 spins with $\xi_W^2 = 1$, as detailed in End Matter. The results show that even with a large number of measurements resulting in a small error bar, statistical fluctuations can still cause a non-spin-squeezed state to be mistakenly classified as spin-squeezed.

Methods — We here focus on null-hypothesis significance testing, with the p-value quantifying the probability of obtaining a Wineland parameter at least as extreme as the value actually observed, under the null hypothesis H_0 that the measured state is non-spin-squeezed. A small p-value thus provides strong evidence against H_0 , suggesting that the observed data is unlikely under the assumption that they result from measurements of a non-spin-squeezed state. To ensure the p-value remains independent of any specific quantum state or statistical distribution, we determine an upper bound by considering all possible non-spin-squeezed states.

To formulate the null-hypothesis significance test, we introduce the normalized spin angular momentum operator $Q_{(\cdot)} = 2J_{(\cdot)}/N$, define the following parameter

$$\Gamma = N\text{Var}(Q_{\vec{n}\perp}) - \langle Q_{\vec{n}} \rangle^2. \quad (3)$$

and use the sample variance and sample mean as unbiased estimators for $\text{Var}(Q_{\vec{n}\perp})$ and $\langle Q_{\vec{n}} \rangle^2$. In the asymptotic limit (infinite measurement repetitions), a spin system is considered spin-squeezed if the corresponding state satisfies $\Gamma < 0$. While Eq. (3) provides a natural alternative criterion for spin squeezing, it involves nonlinear terms. Existing concentration inequalities struggle to effectively account for these nonlinearities, resulting in an overly conservative upper bound on the p-value. As a result, the predicted number of measurements required to achieve a small p-value is overestimated (see Supplemental Material, Secs. II and V).

To address these challenges, we propose a family of parameters

$$\Gamma_c = N\langle Q_{\vec{n}\perp}^2 \rangle - f_{\alpha,\beta}(\langle Q_{\vec{n}\perp} \rangle, \langle Q_{\vec{n}} \rangle), \quad (4)$$

where each element is defined by a fixed value of $c = (\alpha, \beta)$. The function $f_{\alpha,\beta}(x, y)$ is the tangent plan to $Nx^2 + y^2$ at the point $c = (\alpha, \beta) \in [-1, 1]$

$$f_{\alpha,\beta}(x, y) = 2\alpha Nx + 2\beta y - Na^2 - \beta^2. \quad (5)$$

Importantly, $f_{\alpha,\beta}(x, y)$ serves as an affine lower bound for $Nx^2 + y^2$ for any (x, y) and (α, β) . This ensures that $\Gamma_c \geq N\langle Q_{\vec{n}\perp}^2 \rangle - N\langle Q_{\vec{n}\perp} \rangle^2 - \langle Q_{\vec{n}} \rangle^2 = \Gamma$ for any choice of $c = (\alpha, \beta)$. As a result, quantum states satisfying $\Gamma_c < 0$ can be classified as spin-squeezed.

To estimate Γ_c in practice, we consider $M/2$ independent and identically distributed (i.i.d.) repeated processes (M is the total number of experimental repetitions). In each processes i , the system undergoes two independent measurements. In the first measurement, the quantum state is prepared, and a measurement of $Q_{\vec{n}}$ is performed, yielding the outcome $q_{\vec{n}}^{(i)} \in [-1, 1]$. In the second measurement, the quantum state is re-prepared, and a measurement of $Q_{\vec{n}\perp}$ is performed, obtaining the outcome $q_{\vec{n}\perp}^{(i)} \in [-1, 1]$. Using these measurement outcomes, we define the estimator of Γ_c for each experimental processes i as the random variable

$$\tilde{\Gamma}_{c,i} = N \left(q_{\vec{n}\perp}^{(i)} \right)^2 - f_{\alpha,\beta} \left(q_{\vec{n}\perp}^{(i)}, q_{\vec{n}}^{(i)} \right). \quad (6)$$

Given the $M/2$ repetitions, Γ_c can be estimated by using the following statistical estimator

$$\tilde{\Gamma}_c = \frac{2}{M} \sum_{i=1}^{M/2} \tilde{\Gamma}_{c,i}. \quad (7)$$

Let $\gamma_c < 0$ be the observed value of $\tilde{\Gamma}_c$ from a given experimental realization. We are interested in the p-value, i.e. the probability that the estimator $\tilde{\Gamma}_c$ takes a value equal to or smaller than γ_c , assuming the measurements are performed on non-spin-squeezed states (the null hypothesis H_0). We name it explicitly as $P(\tilde{\Gamma}_c \leq \gamma_c | H_0)$. Importantly, $P(\tilde{\Gamma}_c \leq \gamma_c | H_0)$ must be estimated by considering all possible non-spin-squeezed states and all possible statistical distributions. If $P(\tilde{\Gamma}_c \leq \gamma_c | H_0)$ is less than a predetermined significance level, such as 0.05, we conclude that the system of interest exhibits spin squeezing.

Establishing upper bounds on the p-value — Concentration inequalities [29, 30] can be used to upper bound $P(\tilde{\Gamma}_c \leq \gamma_c | H_0)$. As shown in Supplemental Material, Sec. III, the Bernstein inequality for example gives

$$P(\tilde{\Gamma}_c \leq \gamma_c | H_0) \leq \exp \left\{ \frac{\gamma_c^2 M/2}{2\Gamma_1^c \Gamma_0^c + 2(\Gamma_1^c - \Gamma_0^c)\gamma_c/3} \right\} \quad (8)$$

where

$$\Gamma_1^c = \max_{q_{\vec{n}\perp}^{(i)}, q_{\vec{n}}^{(i)}} \tilde{\Gamma}_{c,i} = N(1 + |\alpha|)^2 + (1 + |\beta|)^2 - 1,$$

$$\Gamma_0^c = \min_{q_{\vec{n}\perp}^{(i)}, q_{\vec{n}}^{(i)}} \tilde{\Gamma}_{c,i} = (1 - |\beta|)^2 - 1.$$

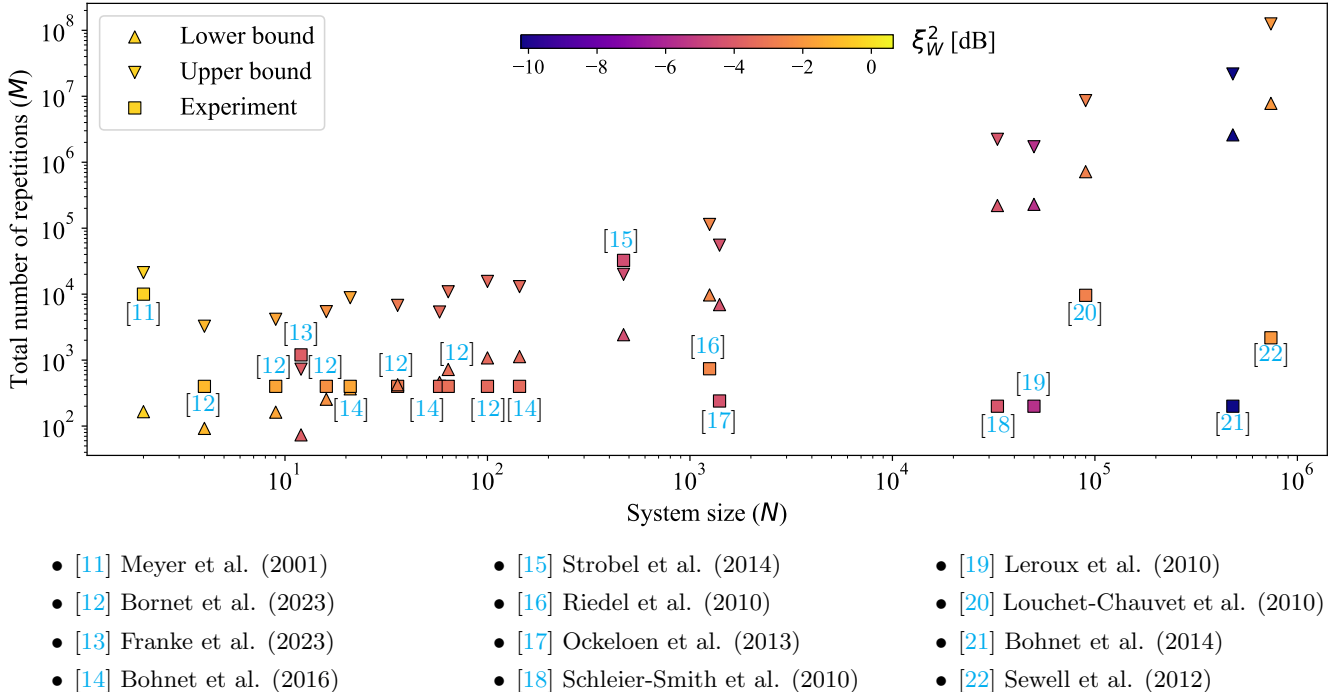


FIG. 1. Experimental achievements together with their statistical analysis. The experiments that have been reported in the literature are identified by a square whose position specifies the total number of experimental repetitions (M) that has been realized and the system size (N). The color of the square gives the observed value of the Wineland parameter. Every square is accompanied by a number used to identify the reference as specified below the graph. The significance of the experimental outcomes are quantified by the number of measurements that are necessary and sufficient to reach a p-value of 5%. Namely, the upper triangle (with the vertex pointing down) gives the total number of measurement repetitions that is sufficient to reject the hypothesis that non-spin squeezed states were measured. The lower triangle (with the vertex pointing up) specifies the number of measurements that is required in order to ensure that a specific non-spin squeezed state (according to the Wineland parameter) cannot reproduce the observed statistics.

The right-hand side of Ineq. (8) is solely a function of the parameter $c = (\alpha, \beta)$ and the experimental observation γ_c . It can be minimized over $c = (\alpha, \beta)$ under the constraint that $\gamma_c < 0$ in order to get the tightest upper bound on the p-value. This defines p_{opt} as

$$p_{\text{opt}} = \inf_{\alpha, \beta \text{ s.t. } \gamma_c < 0} \exp \left\{ \frac{\gamma_c^2 M/2}{2\Gamma_1^c \Gamma_0^c + 2(\Gamma_1^c - \Gamma_0^c)\gamma_c/3} \right\}. \quad (9)$$

Guidelines for robust statistical evidence of spin squeezing in future experiments — We now have all the ingredients to propose a concrete recipe that can be used to establish a robust statistical evidence of spin squeezing in future experiments. First, we consider $M/2$ measurements of both $Q_{\vec{n}}$ and $Q_{\vec{n}\perp}$. This yields outcomes $q_{\vec{n}}^{(i)}$ and $q_{\vec{n}\perp}^{(i)}$ for $i \in [1, M/2]$. γ_c is then deduced from the estimator $\tilde{\Gamma}_c$ given in Eq. (6). An upper bound on the p-value is obtained from the minimization given in Eq. (9) over α and β such that $\gamma_c < 0$. A small p_{opt} provides strong evidence against H_0 , suggesting that the observed data is unlikely under the assumption that they result from measurements of a non-spin-squeezed state.

Analysis of existing experimental realizations — To estimate what could have been achieved in previously implemented experimental realizations, we calculated the value of γ_c from Refs. [11–22] by assuming that $\sum_{i=1}^{M/2} q_{\vec{n}_\perp}^{(i)} = 0$. We increase M , optimizing (α, β) , until the upper bound on the p -value achieves 5%. We then execute numerical simulations to show that the assumption $\sum_{i=1}^{M/2} q_{\vec{n}_\perp}^{(i)} = 0$ is conservative, i.e. it minimizes the number of experimental repetitions that are needed to achieve a given upper bound on the p -value, see Supplemental Material Sec. IV. The value of M that we find is reported in Fig. 1 (triangle with the vertex pointing down) as a function of the system size for each experiment separately. The actual number of experimental repetitions conducted is also indicated (square). Except for the experiment involving 16 spins¹ reported in Ref. [13]

¹ In Ref. [13], the authors specify that each measurement point reported in their paper is an average of 50 to 600 repetitions of experimental realizations. The position of the corresponding square in Fig. 1 assumes that 1200 repetitions in total were per-

and 470 spins² in Ref. [15], we cannot reject the hypothesis that non-spin squeezed states were measured with a p-value less than or equal to 5%. For most experiments, the discrepancy between the actual number of measurements and the number required to achieve an upper bound on the p-value of 5% is at least a factor of 10, and can reach up to 10^4 at the worst case.

Establishing lower bounds on the p-value — The upper bound on the p-value we derived before suggests that the number of experimental repetitions performed may be insufficient to rule out the possibility that non-spin-squeezed states were actually produced in most existing experimental realisations. To substantiate this claim, we follow the approach of Refs. [28, 31] and in particular, we consider the following state

$$\hat{\rho} = r|\chi\rangle\langle\chi| + \frac{1-r}{2}(|\uparrow_{\vec{n}_\perp}\rangle\langle\uparrow_{\vec{n}_\perp}| + |\downarrow_{\vec{n}_\perp}\rangle\langle\downarrow_{\vec{n}_\perp}|) \quad (10)$$

where $|\chi\rangle$ is a squeezed state with mean spin direction \vec{n} , $|\uparrow_{\vec{n}_\perp}\rangle = |\uparrow_{\vec{n}_\perp}\rangle^{\otimes N}$, $|\downarrow_{\vec{n}_\perp}\rangle = |\downarrow_{\vec{n}_\perp}\rangle^{\otimes N}$ and $0 \leq r \leq 1$. The state $\hat{\rho}$ is not considered as being spin squeezed by the Wineland parameter ($\xi_W^2(\hat{\rho}) \geq 1$) for any values of r satisfying

$$r \leq r_{\max} = \frac{1}{2} \left(\kappa + \sqrt{\kappa^2 + \frac{4N}{\langle Q_{\vec{n}} \rangle_{|\chi\rangle}^2}} \right) \quad (11)$$

where $\kappa = \xi_W^2(|\chi\rangle) - N/\langle Q_{\vec{n}} \rangle_{|\chi\rangle}^2$ (see Supplemental Material Sec. VI). When performing M measurements on $\hat{\rho}$ with $r \leq r_{\max}$, the probability to only sample the squeezed state $|\chi\rangle$ occurs with a probability $p = r^M \leq r_{\max}^M = p^*$. Hence, p^* establishes a lower bound on the p-value of a statistical test designed to reject the hypothesis that the measured state is of the form given in Eq. (10) [28, 31].

For each experiment reported in Refs. [11–22], we compute the minimum number of measurements required to ensure that the observed statistics could not be reproduced by a non-spin-squeezed state of the form given by $\hat{\rho}$ with a probability p^* sets to 5%. This is derived from $\log(0.05)/\log(r_{\max})$ where $\xi_W^2(|\chi\rangle)$ and $\langle Q_{\vec{n}} \rangle_{|\chi\rangle}^2$ are fixed to the observed values. The results, reported in Fig. 1, show that for most of the experiments involving more than 100 spins, the proposed non-spin squeezed state reproduces the observed results with a probability exceeding 5%.

Discussion and Conclusion — In this paper, we developed a rigorous analytical framework for detecting spin-squeezed states, with a particular focus on the impact of finite measurement repetitions on the detection results. Specifically, by linearizing ξ_W^2 , we proposed a family of criteria for identifying spin-squeezed states. Using a hypothesis-testing approach, we derived upper bounds on the p-value, which can be used to provide a reliable statistical evidence of spin squeezing.

The effects of finite measurement repetitions have long been overlooked in spin-squeezing detection experiments. Our hypothesis-testing framework reveals that most existing experiments fail to pass the statistical test due to an insufficient number of measurements. This issue becomes particularly severe when the spin number is large, as the required number of measurements needed to reliably reject the null hypothesis increases significantly, often exceeding the practical capabilities of current experimental setups. However, this does not necessarily mean that spin squeezing is absent, but rather that the available data does not provide strong enough statistical support for claiming spin squeezing is produced.

Our analysis provides an estimate of the number of measurements which is necessary (but not sufficient) to reject the null hypothesis. From a specific state, we showed that the p-value is lower bounded by $p^* = r_{\max}^M$ where r_{\max} is specified from the expected values of ξ_W^2 and $\langle Q_{\vec{n}} \rangle$, see Eq. (11). Note that $r_{\max} \geq (\sqrt{N^2 + 4N} - N)/2$ and hence, a number of measurements $M \geq \ln 0.05/\ln[(\sqrt{N^2 + 4N} - N)/2] \sim -N \log(0.05)$ is necessary to achieve a p-value smaller than 5%.

Note that the p-value bounds we proposed in Eq. (9) could likely be improved. For instance, using more refined estimators may yield tighter bounds. Additionally, various concentration inequalities could be explored, and although several have already been tested (see Supplemental Material Sec. V), other choices might offer even stronger bounds. Similarly, while we have tested multiple states to construct the lower bound on the p-value, we cannot rule out the possibility that better states exist for this purpose. Moreover, our statistical method could be extended to quantify finite-size effects on other squeezing or entanglement criteria [32]. We leave these extensions for future work. Nonetheless, our results already offer a solid framework for predicting and accurately assessing the outcomes of future experiments focusing on spin squeezing.

Acknowledgments — We thank Gregoire Misguich for helpful discussions. We acknowledge funding by the European High-Performance Computing Joint Undertaking (JU) under grant agreement No 101018180 and project name HPCQS and by a French national quantum initiative managed by Agence Nationale de la Recherche in the framework of France 2030 with the reference ANR-22-PETQ-0007 and project name EPiQ.

formed, as two measurements directions are involved. Actually, 728 realizations are enough to achieve an upper bound on the p-value of 5%.

² In Ref. [15], a tomography was performed using a total of 32500 experimental realizations. The position of the corresponding square in Fig. 1 hence assumes that 32500 realizations were performed. Actually, 19970 realizations (9985 in each measurement direction) ensure a significance level of 5%.

* These authors contributed equally to this work

[1] V. Giovannetti, S. Lloyd, and L. Maccone, Quantum-enhanced measurements: Beating the standard quantum limit, *Science* **306**, 1330 (2004).

[2] V. Giovannetti, S. Lloyd, and L. Maccone, Advances in quantum metrology, *Nat. Photon.* **5**, 222 (2011).

[3] M. W. Mitchell, J. S. Lundeen, and A. M. Steinberg, Super-resolving phase measurements with a multiphoton entangled state, *Nature* **429**, 161 (2004).

[4] T. Nagata, R. Okamoto, J. L. O'Brien, K. Sasaki, and S. Takeuchi, Beating the standard quantum limit with four-entangled photons, *Science* **316**, 726 (2007).

[5] S. Slussarenko, M. M. Weston, H. M. Chrzanowski, L. K. Shalm, V. B. Verma, S. W. Nam, and G. J. Pryde, Unconditional violation of the shot-noise limit in photonic quantum metrology, *Nat. Photon.* **11**, 700 (2017).

[6] S.-R. Zhao, Y.-Z. Zhang, W.-Z. Liu, J.-Y. Guan, W. Zhang, C.-L. Li, B. Bai, M.-H. Li, Y. Liu, L. You, J. Zhang, J. Fan, F. Xu, Q. Zhang, and J.-W. Pan, Field demonstration of distributed quantum sensing without post-selection, *Phys. Rev. X* **11**, 031009 (2021).

[7] J. Aasi, J. Abadie, B. Abbott, R. Abbott, T. Abbott, M. Abernathy, C. Adams, T. Adams, P. Addesso, R. Adhikari, et al., Enhanced sensitivity of the ligo gravitational wave detector by using squeezed states of light, *Nat. Photon.* **7**, 613 (2013).

[8] X. Guo, C. R. Breum, J. Borregaard, S. Izumi, M. V. Larsen, T. Gehring, M. Christandl, J. S. Neergaard-Nielsen, and U. L. Andersen, Distributed quantum sensing in a continuous-variable entangled network, *Nat. Phys.* **16**, 281 (2020).

[9] M. Tse, H. Yu, N. Kijbunchoo, et al., Quantum-enhanced advanced ligo detectors in the era of gravitational-wave astronomy, *Phys. Rev. Lett.* **123**, 231107 (2019).

[10] Y. Xia, W. Li, W. Clark, D. Hart, Q. Zhuang, and Z. Zhang, Demonstration of a reconfigurable entangled radio-frequency photonic sensor network, *Phys. Rev. Lett.* **124**, 150502 (2020).

[11] V. Meyer, M. A. Rowe, D. Kielpinski, C. A. Sackett, W. M. Itano, C. Monroe, and D. J. Wineland, Experimental demonstration of entanglement-enhanced rotation angle estimation using trapped ions, *Phys. Rev. Lett.* **86**, 5870 (2001).

[12] G. Bornet, G. Emperaiger, C. Chen, B. Ye, M. Block, M. Bintz, J. A. Boyd, D. Barredo, T. Comparin, F. Mezzacapo, T. Roscilde, T. Lahaye, N. Y. Yao, and A. Browaeys, Scalable spin squeezing in a dipolar rydberg atom array, *Nature* **621**, 728–733 (2023).

[13] J. Franke, S. R. Muleady, R. Kauberger, F. Kranzl, R. Blatt, A. M. Rey, M. K. Joshi, and C. F. Roos, Quantum-enhanced sensing on optical transitions through finite-range interactions, *Nature* **621**, 740–745 (2023).

[14] J. G. Bohnet, B. C. Sawyer, J. W. Britton, M. L. Wall, A. M. Rey, M. Foss-Feig, and J. J. Bollinger, Quantum spin dynamics and entanglement generation with hundreds of trapped ions, *Science* **352**, 1297–1301 (2016).

[15] H. Strobel, W. Muessel, D. Linnemann, T. Zibold, D. B. Hume, L. Pezzè, A. Smerzi, and M. K. Oberthaler, Fisher information and entanglement of non-gaussian spin states, *Science* **345**, 424–427 (2014).

[16] M. F. Riedel, P. Böhi, Y. Li, T. W. Hänsch, A. Sinatra, and P. Treutlein, Atom-chip-based generation of entanglement for quantum metrology, *Nature* **464**, 1170–1173 (2010).

[17] C. F. Ockeloen, R. Schmied, M. F. Riedel, and P. Treutlein, Quantum metrology with a scanning probe atom interferometer, *Phys. Rev. Lett.* **111**, 143001 (2013).

[18] M. H. Schleier-Smith, I. D. Leroux, and V. Vuletić, States of an ensemble of two-level atoms with reduced quantum uncertainty, *Phys. Rev. Lett.* **104**, 073604 (2010).

[19] I. D. Leroux, M. H. Schleier-Smith, and V. Vuletić, Implementation of cavity squeezing of a collective atomic spin, *Phys. Rev. Lett.* **104**, 073602 (2010).

[20] A. Louchet-Chauvet, J. Appel, J. J. Renema, D. Oblak, N. Kjaergaard, and E. S. Polzik, Entanglement-assisted atomic clock beyond the projection noise limit, *New J. Phys.* **12**, 065032 (2010).

[21] J. G. Bohnet, K. C. Cox, M. A. Norcia, J. M. Weiner, Z. Chen, and J. K. Thompson, Reduced spin measurement back-action for a phase sensitivity ten times beyond the standard quantum limit, *Nat. Photon.* **8**, 731–736 (2014).

[22] R. J. Sewell, M. Koschorreck, M. Napolitano, B. Du-boost, N. Behbood, and M. W. Mitchell, Magnetic sensitivity beyond the projection noise limit by spin squeezing, *Phys. Rev. Lett.* **109**, 253605 (2012).

[23] D. J. Wineland, J. J. Bollinger, W. M. Itano, F. L. Moore, and D. J. Heinzen, Spin squeezing and reduced quantum noise in spectroscopy, *Phys. Rev. A* **46**, R6797 (1992).

[24] M. Kitagawa and M. Ueda, Squeezed spin states, *Phys. Rev. A* **47**, 5138 (1993).

[25] L.-M. Duan, Many-particle entanglement with bose-einstein condensates, *Nature* **409**, 63 (2001).

[26] M. Krzywinski and N. Altman, Error bars, *Nature Methods* **10**, 921 (2013).

[27] S. Wagner, R. Schmied, M. Fadel, P. Treutlein, N. Sangouard, and J.-D. Bancal, Bell correlations in a many-body system with finite statistics, *Phys. Rev. Lett.* **119**, 170403 (2017).

[28] J. L. Bönsel, S. Imai, Y.-C. Liu, and O. Gühne, Error estimation of different schemes to measure spin-squeezing inequalities, *Phys. Rev. A* **110**, 022410 (2024).

[29] C. McDiarmid, On the method of bounded differences, in *Surveys in Combinatorics, 1989* (Cambridge University Press, 1989) p. 148–188.

[30] C. McDiarmid, Concentration, in *Probabilistic Methods for Discrete Math.*, edited by M. Habib, C. McDiarmid, J. Ramirez-Alfonsin, and B. Reed (Springer Berlin Heidelberg, Berlin, Heidelberg, 1998) pp. 195–248.

[31] R. Schmied, J.-D. Bancal, B. Allard, M. Fadel, V. Scarani, P. Treutlein, and N. Sangouard, Bell correlations in a bose-einstein condensate, *Science* **352**, 441 (2016).

[32] L. Pezzè, A. Smerzi, M. K. Oberthaler, R. Schmied, and P. Treutlein, Quantum metrology with nonclassical states of atomic ensembles, *Rev. Mod. Phys.* **90**, 035005 (2018).

[33] F. Becca and S. Sorella, *Quantum Monte Carlo approaches for correlated systems* (Cambridge University Press, 2017).

End Matter

In experimental estimations of the Wineland parameter, standard error bars reflect only the statistical variability of the measured data and do not rigorously quantify the likelihood that the observed statistics could originate from non-spin-squeezed states. To highlight this limitation, we performed Monte Carlo simulations on a specific non-spin-squeezed state, demonstrating explicitly that small error bars do not necessarily correspond to small p-values. This reveals the potential risk of misclassifying non-spin-squeezed states as spin-squeezed when relying solely on error bar.

Specifically, we consider quantum states of the form given by Eq. (10)

$$\hat{\rho} = r |\chi\rangle \langle \chi| + \frac{1-r}{2} (|\uparrow_{\vec{n}_\perp}\rangle \langle \uparrow_{\vec{n}_\perp}| + |\downarrow_{\vec{n}_\perp}\rangle \langle \downarrow_{\vec{n}_\perp}|) \quad (\text{A.12})$$

where $|\chi\rangle$ is generated via an appropriate time evolution under a dipolar XY Hamiltonian (see Supplemental Material Sec. I). In our simulations, we use a square lattice of $N = 9$ spins and obtain a spin-squeezed state characterized by $\xi_W^2(|\chi\rangle) \approx 0.41036$, a mean spin polarization $\langle 2J_y/N \rangle_\chi \approx 0.80812$, and a variance $\text{Var}(2J_x/N)_\chi \approx 0.02977$. From the value of $\xi_W^2(|\chi\rangle)$, we construct a non-spin-squeezed state $\hat{\rho}$ satisfying $\xi_W^2(\hat{\rho}) = 1$, corresponding to parameters $r \approx 0.96154$, $\langle 2J_y/N \rangle_\rho \approx 0.77704$ and $\text{Var}(2J_x/N)_\rho \approx 0.06709$.

The statistics that would be obtained from such a state are generated using Monte Carlo sampling. Two data sets, each of size $M/2$, are produced (M is the total number of samples). The first data set, $Q_y = \{y_1, \dots, y_{M/2}\}$, is sampled in the eigenbasis of $2J_y/N$. The second data set, $Q_x = \{x_1, \dots, x_{M/2}\}$, is sampled in the eigenbasis of $2J_x/N$. To establish a comprehensive error estimation framework, the measurement outcomes x_i and y_j are assumed to be independent and identically distributed (i.i.d.). Their (unknown) true means are labeled (μ_x, μ_y) and true variances by (σ_x^2, σ_y^2) .

Recalling the definition of the Wineland parameter from Eq. (2), it can be conveniently rewritten as

$$\xi_W^2 = \frac{N(\mu_{x^2} - \mu_x^2)}{\mu_y^2}, \quad (\text{A.13})$$

where μ_{x^2} is the true mean of the second-order moment of x_i which satisfies $\mu_{x^2} = \sigma_x^2 + \mu_x^2$. A natural approach to estimate ξ_W^2 in practice is to substitute the true expectations by the sample means. However, this introduces a systematic bias due to the nonlinear dependence on μ_x and μ_y [33]. To mitigate this issue, the jackknife method can be used [13, 15]. Specifically, the bias-corrected jack-

knife estimation of ξ_W^2 is given by (see Supplemental Material Sec I)

$$\frac{M}{2} \xi_W^2(\bar{x}, \bar{x^2}, \bar{y}) - \left(\frac{M}{2} - 1 \right) \bar{[\xi_W^2]}, \quad (\text{A.14})$$

where $\bar{x} = \frac{1}{M/2} \sum_{i=1}^{M/2} x_i$, $\bar{x^2} = \frac{1}{M/2} \sum_{i=1}^{M/2} x_i^2$, $\bar{y} = \frac{1}{M/2} \sum_{i=1}^{M/2} y_i$ are the sample means of datasets. $\bar{[\xi_W^2]}$ is the mean of jackknife replicates, defined as $\bar{[\xi_W^2]} = \frac{1}{M/2} \sum_{i=1}^{M/2} \xi_W^2([x]_i, [x^2]_i, [y]_i)$ with $[x]_i = \frac{1}{M/2-1} \sum_{j \neq i} x_j$, $[y]_i = \frac{1}{M/2-1} \sum_{j \neq i} y_j$ the jackknife leave-one-out averages.

The uncertainty in the jackknife estimation is quantified by the error bar

$$\sqrt{M/2 - 1} \times \sqrt{\bar{[\xi_W^2]}^2 - (\bar{[\xi_W^2]})^2}, \quad (\text{A.15})$$

where the second moment of the jackknife replicates is given by $\bar{[\xi_W^2]}^2 = \frac{1}{M/2} \sum_{i=1}^{M/2} [\xi_W^2([x]_i, [x^2]_i, [y]_i)]^2$. This error bar scales as $O(1/\sqrt{M/2})$, substantially exceeding the bias in the estimate (see Supplemental Material Sec. I).

Figure 2 shows the results of the Monte Carlo simulation with the jackknife estimation and uncertainty with one standard error, i.e.

$$\begin{aligned} \widetilde{\xi_W^2} &= (M/2) \xi_W^2(\bar{x}, \bar{x^2}, \bar{y}) - (M/2 - 1) \bar{[\xi_W^2]} \quad (\text{A.16}) \\ &\pm \sqrt{M/2 - 1} \times \sqrt{\bar{[\xi_W^2]}^2 - (\bar{[\xi_W^2]})^2} \end{aligned}$$

as a function of the total number of samples M . Although these values fluctuate around the true value $\xi_W^2 = 1$, some are noticeably below 1. For instance, for $M = 400$, we observe $\widetilde{\xi_W^2} = 0.65832 \pm 0.13115$, despite the data being generated by a non-spin-squeezed state. The same figure also displays the p-value as a function of the number of measurements. None of the p-value drops below 0.25037. In particular, the p-value for $M = 400$ is below 0.66661 clearly indicating a high probability that the measured state is non-spin-squeezed. More generally, none of these results can pass the hypothesis test and thus do not provide statistically significant evidence for spin squeezing. These simulation results (see also the complementary results presented in Supplemental Material Sec. I) emphasize that “error bars primarily quantify the spread of the data or the precision of the mean estimate, but do not constitute a rigorous test for statistical significance [26]”. Therefore, to provide a more reliable assessment of spin squeezing, it is essential to incorporate p-values as a complementary statistical measure to properly evaluate the probability that a non-spin squeezed state reproduces the observed statistics.

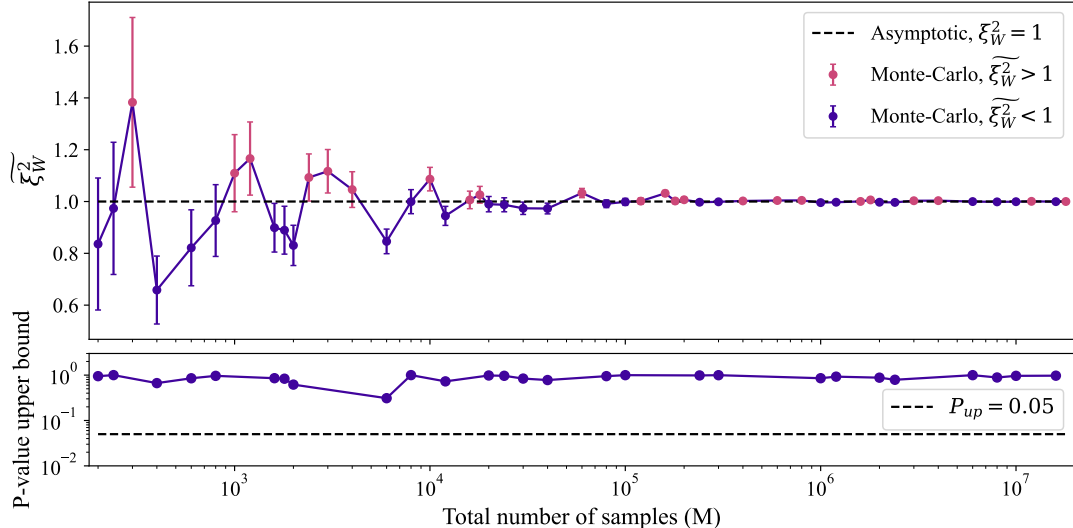


FIG. 2. (Top) Estimation of the Wineland parameter from Monte Carlo samples of size M sampled from a non-spin-squeezed state. Two data sets were sampled: one in the eigenbasis of the mean spin direction (J_y) and another in the eigenbasis of the squeezing axis. Each error bar corresponds to one standard deviation. (Bottom) P-value upper bound using the method proposed in the main text on the Monte-Carlo samples.

Supplemental Material: Testing the Wineland Criterion with Finite Statistics

E. S. Carrera,* Y. Zhang,* J-D. Bancal, and N. Sangouard

Université Paris-Saclay, CEA, CNRS, Institut de physique théorique, 91191, Gif-sur-Yvette, France

(Dated: May 6, 2025)

I. MISCLASSIFICATION OF NON-SPIN-SQUEEZED STATES USING ERROR BAR METHODS

We here review standard error bar estimation methods and discuss in particular, how they apply to the Wineland parameter. Importantly, we emphasize that the error bar solely reflects the statistical spread of the data and does not quantify the likelihood that the observed data could be reproduced by non-spin-squeezed states. This is illustrated in End Matter from the statistics of a non-spin-squeezed state obtained with Monte Carlo techniques by explicitly showing that small error bars do not necessarily correspond to small p-values. This underscores the risk of misclassifying a non-spin-squeezed state as spin-squeezed when relying on error bars to assess the significance of experimental results.

A. Statistics of a non spin-squeezed state

We consider the statistics that would be produced from states of the form

$$\hat{\rho} = r |\chi\rangle \langle \chi| + \frac{1-r}{2} (|\uparrow_{\vec{n}_\perp}\rangle \langle \uparrow_{\vec{n}_\perp}| + |\downarrow_{\vec{n}_\perp}\rangle \langle \downarrow_{\vec{n}_\perp}|) \quad (\text{S-1})$$

where $|\chi\rangle$ is a squeezed state with mean spin direction \vec{n} , $|\uparrow_{\vec{n}_\perp}\rangle = |\uparrow_{\vec{n}_\perp}\rangle^{\otimes N}$, $|\downarrow_{\vec{n}_\perp}\rangle = |\downarrow_{\vec{n}_\perp}\rangle^{\otimes N}$ and $0 \leq r \leq 1$. Inspired by two-axis twisting methods recently applied in Rydberg atom quantum simulators, $|\chi\rangle$ is generated from the time evolution of a coherent spin state under a dipolar XY model Hamiltonian

$$H_{\text{XY}} = J \sum_{i < j} \frac{a^3}{r_{ij}^3} (S_i^x S_j^x + S_i^y S_j^y), \quad (\text{S-2})$$

where S_i^α are the spin-1/2 Pauli operators, r_{ij} is the distance between spin i and j , J denotes the dipolar interaction strength, and a is the lattice spacing. We consider in particular, a square array of $N = 9$ spin-1/2 particles, initially prepared in a coherent spin-squeezed state aligned along the y -axis. The result of a time-evolution simulation using the library *DynamiQs* [1] shows a spin-squeezed state with squeezing direction \vec{x} and mean spin direction \vec{y} characterized by $\xi_W^2(|\chi\rangle) \approx 0.41036$, $\langle 2J_y/N \rangle_\chi \approx 0.80812$ and $\text{Var}(2J_x/N)_\chi \approx 0.02977$ at time $t \approx 0.20707/J$. Using this state, we construct a non-spin-squeezed state satisfying $\xi_W^2(\rho) = 1$, which is characterized by $r \approx 0.96154$, $\langle 2J_y/N \rangle_\rho \approx 0.77704$ and $\text{Var}(2J_x/N)_\rho \approx 0.06709$.

The statistics that would be obtained from such a state are generated using Monte Carlo sampling. Two data sets, each of size $M/2$, are produced (M is the total number of samples). The first data set, $Q_y = \{y_1, \dots, y_{M/2}\}$, is sampled in the eigenbasis of $2J_y/N$. The second data set, $Q_x = \{x_1, \dots, x_{M/2}\}$, is sampled in the eigenbasis of $2J_x/N$. To establish a comprehensive error estimation framework, the measurement outcomes x_i and y_j are assumed to be independent and identically distributed (i.i.d.).

Although the underlying probability distributions of x_i and y_i are generally unknown, we define their true expectations as $\mu_x = \langle x_i \rangle$ and $\mu_y = \langle y_i \rangle$, and their true variances as $\sigma_x^2 = \langle (x_i - \mu_x)^2 \rangle$ and $\sigma_y^2 = \langle (y_i - \mu_y)^2 \rangle$. Here, the notation $\langle \dots \rangle$ represents the true expectation over the unknown underlying distribution, which is a quantity that cannot be directly observed in practice. In our analysis, we further consider the second-order moment of x_i and used $\mu_{x^2} = \langle x_i^2 \rangle$ to label its true expectation. Note that $\mu_{x^2} = \sigma_x^2 + \mu_x^2$. With these quantities at hand, the Wineland parameter ξ_W^2 can be expressed as

$$\xi_W^2 = \frac{N[\mu_{x^2} - (\mu_x)^2]}{(\mu_y)^2}. \quad (\text{S-3})$$

* These authors contributed equally to this work

To estimate the Wineland parameter from a given dataset Q_x and Q_y , it is essential to obtain empirical estimates of μ_x , μ_{x^2} and μ_y . Since the true means and variances of the underlying distributions are not directly accessible, we estimate them using their sample counterparts, which are computed from a finite number of observations. We begin by defining the sample means of the data sets Q_x and Q_y , denoted as \bar{x} and \bar{y} , respectively. Here, the overbar notation $\overline{\cdots}$ represents the sample mean computed from $M/2$ data points. In addition, we introduce the sample variance s_x^2 and s_y^2 , which quantify the spread of the data, as well as the second raw moment of Q_x (mean square), denoted as $\overline{x^2}$. These quantities are given by

$$\begin{aligned}\bar{x} &= \frac{1}{M/2} \sum_{i=1}^{M/2} x_i, & s_x^2 &= \frac{1}{M/2-1} \sum_{i=1}^{M/2} (x_i - \bar{x})^2, & \overline{x^2} &= \frac{1}{M/2} \sum_{i=1}^{M/2} x_i^2 \\ \bar{y} &= \frac{1}{M/2} \sum_{i=1}^{M/2} y_i, & s_y^2 &= \frac{1}{M/2-1} \sum_{i=1}^{M/2} (y_i - \bar{y})^2.\end{aligned}\quad (\text{S-4})$$

We have

$$\begin{aligned}\langle \bar{x} \rangle &= \frac{1}{M/2} \sum_{i=1}^{M/2} \langle x_i \rangle = \mu_x, & \sigma_x^2 &= \langle s_x^2 \rangle, & \langle \overline{x^2} \rangle &= \frac{1}{M/2} \sum_{i=1}^{M/2} \langle x_i^2 \rangle = \sigma_x^2 + \mu_x^2 = \mu_{x^2}, \\ \langle \bar{y} \rangle &= \frac{1}{M/2} \sum_{i=1}^{M/2} \langle y_i \rangle = \mu_y, & \sigma_y^2 &= \langle s_y^2 \rangle.\end{aligned}\quad (\text{S-5})$$

These results indicate that the sample means \bar{x} , $\overline{x^2}$ and \bar{y} serve as unbiased estimators of their respective true expectations μ_x , μ_{x^2} and μ_y . Likewise, the sample variances s_x^2 and s_y^2 provide unbiased estimators of the true variances σ_x^2 and σ_y^2 , ensuring that, on average, these estimates converge to their theoretical counterparts as the sample size increases.

Using these empirical quantities, the most natural approach to estimate ξ_W^2 is to approximate the true expectation by their sample counterparts, namely, setting $\mu_x \approx \bar{x}$, $\mu_y \approx \bar{y}$ and $\mu_{x^2} \approx \overline{x^2}$. However, due to the nonlinear nature of ξ_W^2 , this direct substitution will introduce a systematic bias in the estimation [2]. To mitigate this issue, experimental studies often employ statistical techniques such as error propagation [3], the bootstrap method, or the jackknife method [4, 5] to assess and correct for biases introduced by nonlinear transformations. In this work, we focus on the jackknife resampling technique, which will be introduced in subsequent sections. This method provides an effective means of quantifying the bias arising from finite sample effects and improving the accuracy of the estimated Wineland parameter.

B. Estimating the Wineland parameter with the Jackknife Method

The jackknife resampling method [2] is a widely used statistical technique for estimating uncertainties in nonlinear functions. It provides a systematic and fully automated approach to determining both error bars and bias corrections.

Proposition 1. Consider three independent datasets, each consisting of L i.i.d. random variables, $\{u_1, \dots, u_L\}$, $\{v_1, \dots, v_L\}$, and $\{w_1, \dots, w_L\}$. The corresponding true means and variances are denoted as μ_u, μ_v, μ_w and $\sigma_u^2, \sigma_v^2, \sigma_w^2$, respectively. Let the sample means of the datasets be denoted as $\bar{u} = \frac{1}{L} \sum_{i=1}^L u_i$, $\bar{v} = \frac{1}{L} \sum_{i=1}^L v_i$ and $\bar{w} = \frac{1}{L} \sum_{i=1}^L w_i$. Let $\{[u]_i\}$, $\{[v]_i\}$, and $\{[w]_i\}$ be the Jackknife datasets, where $[\cdot]_i$ is the jackknife averages computed by systematically leaving out the i -th data point from the original dataset, i.e., $[u]_i = \frac{1}{L} \sum_{j \neq i} u_j$, $[v]_i = \frac{1}{L} \sum_{j \neq i} v_j$, $[w]_i = \frac{1}{L} \sum_{j \neq i} w_j$. Let $\overline{[\cdot]} = \frac{1}{L} \sum_{i=1}^L [\cdot]_i$ be the sample mean of the jackknife averages, and $[\cdot]^2 = \frac{1}{L} \sum_{i=1}^L [\cdot]_i^2$ the second raw moment. For any differentiable function f , denoting the i -th jackknife estimates of f as $[f]_i = f([u]_i, [v]_i, [w]_i)$, the jackknife estimate of $f(\mu_u, \mu_v, \mu_w)$ is then given by

$$Lf(\bar{u}, \bar{v}, \bar{w}) - (L-1)\overline{[f]}, \quad (\text{S-6})$$

where $\overline{[f]} = \frac{1}{L} \sum_{i=1}^L [f]_i$ is the mean of jackknife estimates. For the variance of $f(\mu_u, \mu_v, \mu_w)$, it is estimated by

$$(L-1) \left(\overline{[f]^2} - \overline{[f]}^2 \right), \quad (\text{S-7})$$

where $\overline{[f]^2} - \left(\overline{[f]}\right)^2 = s_{[f]}^2$ is the jackknife variance of the jackknife estimates. The bias of the jackknife estimate of $f(\mu_u, \mu_v, \mu_w)$ scales as $O(1/L)$, while the estimated error bar $\sqrt{(L-1)s_{[f]}^2}$ scales as $O(1/\sqrt{L})$.

Proof. We begin by identifying the leading-order contributions to the bias in the estimation of $f(\mu_u, \mu_v, \mu_w)$. Due to the nonlinear nature of f , direct substitution of the true means by the sample means generally introduces a systematic bias. To quantify this effect, we expand $f(\bar{u}, \bar{v}, \bar{w})$ around its expectation at the true mean values, $f(\mu_u, \mu_v, \mu_w)$, using a multivariate Taylor series expansion, retaining terms up to the second order. We get

$$\begin{aligned} f(\bar{u}, \bar{v}, \bar{w}) &= f(\mu_u, \mu_v, \mu_w) + (\partial_{\mu_u} f) \Delta_u + (\partial_{\mu_v} f) \Delta_v + (\partial_{\mu_w} f) \Delta_w \\ &\quad + \frac{1}{2} (\partial_{\mu_u, \mu_u}^2 f) \Delta_u^2 + \frac{1}{2} (\partial_{\mu_v, \mu_v}^2 f) \Delta_v^2 + \frac{1}{2} (\partial_{\mu_w, \mu_w}^2 f) \Delta_w^2 \\ &\quad + (\partial_{\mu_u, \mu_v}^2 f) \Delta_u \Delta_v + (\partial_{\mu_u, \mu_w}^2 f) \Delta_u \Delta_w + (\partial_{\mu_v, \mu_w}^2 f) \Delta_v \Delta_w, \end{aligned} \quad (\text{S-8})$$

where $\Delta_u = \bar{u} - \mu_u$, $\Delta_v = \bar{v} - \mu_v$ and $\Delta_w = \bar{w} - \mu_w$. The leading contribution to the bias comes from the second-order terms, since the first-order terms in Δ_u , Δ_v , and Δ_w have zero expectation, i.e., $\langle \Delta_u \rangle = 0$, $\langle \Delta_v \rangle = 0$, and $\langle \Delta_w \rangle = 0$. Instead, the second-order terms have finite expectation values

$$\begin{aligned} \langle \Delta_u^2 \rangle &= \langle \bar{u}^2 \rangle - \langle \bar{u} \rangle^2 = \sigma_{\bar{u}}^2 = \frac{\sigma_u^2}{L}, \quad \langle \Delta_v^2 \rangle = \langle \bar{v}^2 \rangle - \langle \bar{v} \rangle^2 = \sigma_{\bar{v}}^2 = \frac{\sigma_v^2}{L}, \quad \langle \Delta_w^2 \rangle = \langle \bar{w}^2 \rangle - \langle \bar{w} \rangle^2 = \sigma_{\bar{w}}^2 = \frac{\sigma_w^2}{L}, \\ \langle \Delta_u \Delta_v \rangle &= \langle \bar{u} \bar{v} \rangle - \langle \bar{u} \rangle \langle \bar{v} \rangle = \sigma_{\bar{u} \bar{v}}^2 = \frac{\sigma_{uv}^2}{L}, \quad \langle \Delta_u \Delta_w \rangle = \langle \bar{u} \bar{w} \rangle - \langle \bar{u} \rangle \langle \bar{w} \rangle = \sigma_{\bar{u} \bar{w}}^2 = \frac{\sigma_{uw}^2}{L}, \\ \langle \Delta_v \Delta_w \rangle &= \langle \bar{v} \bar{w} \rangle - \langle \bar{v} \rangle \langle \bar{w} \rangle = \sigma_{\bar{v} \bar{w}}^2 = \frac{\sigma_{vw}^2}{L}. \end{aligned} \quad (\text{S-9})$$

Here, σ_{uv} , σ_{uw} and σ_{vw} are the covariance. Substituting these expressions into the Taylor expansion, we obtain

$$\begin{aligned} \langle f(\bar{u}, \bar{v}, \bar{w}) \rangle - f(\mu_u, \mu_v, \mu_w) &= \frac{1}{2L} \left[(\partial_{\mu_u, \mu_u}^2 f) \sigma_u^2 + (\partial_{\mu_v, \mu_v}^2 f) \sigma_v^2 + (\partial_{\mu_w, \mu_w}^2 f) \sigma_w^2 \right] \\ &\quad + \frac{1}{L} \left[(\partial_{\mu_u, \mu_v}^2 f) \sigma_{uv}^2 + (\partial_{\mu_u, \mu_w}^2 f) \sigma_{uw}^2 + (\partial_{\mu_v, \mu_w}^2 f) \sigma_{vw}^2 \right], \end{aligned} \quad (\text{S-10})$$

which proves that the leading bias in estimating $f(\mu_u, \mu_v, \mu_w)$ from $f(\bar{u}, \bar{v}, \bar{w})$ is of order $O(1/L)$.

We now establish the jackknife estimate for $f(\mu_u, \mu_v, \mu_w)$. We first extend S-10 formally to get second order contributions, that is, we write

$$f(\mu_u, \mu_v, \mu_w) = \langle f(\bar{u}, \bar{v}, \bar{w}) \rangle - \frac{A_\sigma}{L} + \frac{B_\sigma}{L^2}, \quad (\text{S-11})$$

where A_σ/L and B_σ/L^2 are the first and second order contributions to the bias. From S-10, we have

$$A_\sigma = \frac{1}{2} \left[(\partial_{\mu_u, \mu_u}^2 f) \sigma_u^2 + (\partial_{\mu_v, \mu_v}^2 f) \sigma_v^2 + (\partial_{\mu_w, \mu_w}^2 f) \sigma_w^2 \right] + (\partial_{\mu_u, \mu_v}^2 f) \sigma_{uv}^2 + (\partial_{\mu_u, \mu_w}^2 f) \sigma_{uw}^2 + (\partial_{\mu_v, \mu_w}^2 f) \sigma_{vw}^2. \quad (\text{S-12})$$

To derive the jackknife estimator, we expand each leave-one-out estimate $[f]_i$ around $f(\mu_u, \mu_v, \mu_w)$,

$$\begin{aligned} \overline{[f]} &= f(\mu_u, \mu_v, \mu_w) + (\partial_{\mu_u} f)(\bar{u} - \mu_u) + (\partial_{\mu_v} f)(\bar{v} - \mu_v) + (\partial_{\mu_w} f)(\bar{w} - \mu_w) \\ &\quad + \frac{(\partial_{\mu_u, \mu_u}^2 f)}{2L} \sum_{i=1}^L ([u]_i - \mu_u)^2 + \frac{(\partial_{\mu_v, \mu_v}^2 f)}{2L} \sum_{i=1}^L ([v]_i - \mu_v)^2 + \frac{(\partial_{\mu_w, \mu_w}^2 f)}{2L} \sum_{i=1}^L ([w]_i - \mu_w)^2 \\ &\quad + \frac{(\partial_{\mu_u, \mu_v}^2 f)}{L} \sum_{i=1}^L ([u]_i - \mu_u)([v]_i - \mu_v) + \frac{(\partial_{\mu_u, \mu_w}^2 f)}{L} \sum_{i=1}^L ([u]_i - \mu_u)([w]_i - \mu_w) + \frac{(\partial_{\mu_v, \mu_w}^2 f)}{L} \sum_{i=1}^L ([v]_i - \mu_v)([w]_i - \mu_w) \\ &\quad + O\left(\frac{1}{L^2}\right). \end{aligned} \quad (\text{S-13})$$

For the sums, we use the following identities

$$\begin{aligned} \frac{1}{L} \sum_{i=1}^L ([u]_i - \mu_u)^2 &= (\bar{u} - \mu_u)^2 + \frac{s_u^2}{L(L-1)} \\ \frac{1}{L} \sum_{i=1}^L ([u]_i - \mu_u)([v]_i - \mu_v) &= (\bar{u} - \mu_u)(\bar{v} - \mu_v) + \frac{s_{uv}^2}{L(L-1)}. \end{aligned} \quad (\text{S-14})$$

Here, s_{uv}^2 denotes the sample covariance

$$s_{uv}^2 = \frac{1}{L-1} \sum_{i=1}^L (u_i - \bar{u})(v_i - \bar{v}), \quad (\text{S-15})$$

which is an unbiased estimator for the covariance σ_{uv}^2 . Similar expressions hold for the other summation terms. Substituting these and taking the expectation of S-13, the jackknife expansion is given by

$$f(\mu_u, \mu_v, \mu_w) = \langle \bar{f} \rangle - \frac{A_\sigma}{L-1} + \frac{B'_\sigma}{(L-1)^2}. \quad (\text{S-16})$$

Here, the next order correction is represented by B'_σ , which is different from B_σ due to the jackknife averages. We can therefore eliminate the leading contribution to the bias by forming an appropriate linear combination of S-11 and S-16, that is

$$f(\mu_u, \mu_v, \mu_w) = L\langle f(\bar{u}, \bar{v}, \bar{w}) \rangle - (L-1)\langle \bar{f} \rangle + \frac{B_\sigma}{L} - \frac{B'_\sigma}{L-1}. \quad (\text{S-17})$$

Consequently, to eliminate the leading bias without computing partial derivatives, we estimate $f(\mu_u, \mu_v, \mu_w)$ by

$$Lf(\bar{u}, \bar{v}, \bar{w}) - (L-1)\bar{f}. \quad (\text{S-18})$$

Next, we analyze the leading contributions to the statistical uncertainty. The variance σ_f^2 of the estimate $f(\bar{u}, \bar{v}, \bar{w})$ is defined as [2]

$$\begin{aligned} \sigma_f^2 &= \langle f(\bar{u}, \bar{v}, \bar{w})^2 \rangle - \langle f(\bar{u}, \bar{v}, \bar{w}) \rangle^2 = \langle [f(\bar{u}, \bar{v}, \bar{w}) - \langle f(\bar{u}, \bar{v}, \bar{w}) \rangle]^2 \rangle = \langle [f(\bar{u}, \bar{v}, \bar{w}) - f(\mu_u, \mu_v, \mu_w)]^2 \rangle \\ &= \frac{1}{L} [(\partial_{\mu_u} f)^2 \sigma_u^2 + (\partial_{\mu_v} f)^2 \sigma_v^2 + (\partial_{\mu_w} f)^2 \sigma_w^2] + \frac{2}{L} [(\partial_{\mu_u} f)(\partial_{\mu_v} f) \sigma_{uv}^2 + (\partial_{\mu_u} f)(\partial_{\mu_w} f) \sigma_{uw}^2 + (\partial_{\mu_v} f)(\partial_{\mu_w} f) \sigma_{vw}^2]. \end{aligned} \quad (\text{S-19})$$

where, to get the last line, we omitted all second-order terms in S-8 as they contribute at the $O(1/L^2)$ level. Interestingly, the jackknife method can estimate σ_f^2 without requiring explicit computation of partial derivatives. To demonstrate this, we expand each $[f]_i$ around $f(\mu_u, \mu_v, \mu_w)$ and include only the leading contribution, which gives,

$$\bar{f} - f(\mu_u, \mu_v, \mu_w) = (\partial_{\mu_u} f)(\bar{u} - \mu_u) + (\partial_{\mu_v} f)(\bar{v} - \mu_v) + (\partial_{\mu_w} f)(\bar{w} - \mu_w). \quad (\text{S-20})$$

Similarly, for the second moment, we have

$$\begin{aligned} \bar{f}^2 &= \frac{1}{L} \sum_{i=1}^L [f(\mu_u, \mu_v, \mu_w) + (\partial_{\mu_u} f)([u]_i - \mu_u) + (\partial_{\mu_v} f)([v]_i - \mu_v) + (\partial_{\mu_w} f)([w]_i - \mu_w)]^2 \\ &= f^2(\mu_u, \mu_v, \mu_w) + 2f(\mu_u, \mu_v, \mu_w) [(\partial_{\mu_u} f)(\bar{u} - \mu_u) + (\partial_{\mu_v} f)(\bar{v} - \mu_v) + (\partial_{\mu_w} f)(\bar{w} - \mu_w)] \\ &\quad + (\partial_{\mu_u} f)^2 \left[(\bar{u} - \mu_u)^2 + \frac{s_u^2}{L(L-1)} \right] + (\partial_{\mu_v} f)^2 \left[(\bar{v} - \mu_v)^2 + \frac{s_v^2}{L(L-1)} \right] + (\partial_{\mu_w} f)^2 \left[(\bar{w} - \mu_w)^2 + \frac{s_w^2}{L(L-1)} \right] \\ &\quad + 2(\partial_{\mu_u} f)(\partial_{\mu_v} f) \left[(\bar{u} - \mu_u)(\bar{v} - \mu_v) + \frac{s_{uv}^2}{L(L-1)} \right] + 2(\partial_{\mu_u} f)(\partial_{\mu_w} f) \left[(\bar{u} - \mu_u)(\bar{w} - \mu_w) + \frac{s_{uw}^2}{L(L-1)} \right] \\ &\quad + 2(\partial_{\mu_v} f)(\partial_{\mu_w} f) \left[(\bar{v} - \mu_v)(\bar{w} - \mu_w) + \frac{s_{vw}^2}{L(L-1)} \right]. \end{aligned} \quad (\text{S-21})$$

Hence, the variance in the jackknife estimates is given by

$$\begin{aligned} s_{[f]}^2 &= \bar{f}^2 - \langle \bar{f} \rangle^2 = \frac{1}{L(L-1)} [(\partial_{\mu_u} f)^2 s_u^2 + (\partial_{\mu_v} f)^2 s_v^2 + (\partial_{\mu_w} f)^2 s_w^2] \\ &\quad + \frac{2}{L(L-1)} [(\partial_{\mu_u} f)(\partial_{\mu_v} f) s_{uv}^2 + (\partial_{\mu_u} f)(\partial_{\mu_w} f) s_{uw}^2 + (\partial_{\mu_v} f)(\partial_{\mu_w} f) s_{vw}^2]. \end{aligned} \quad (\text{S-22})$$

Taking the expectation and comparing with the variance given in Eq. S-19, we obtain

$$\langle s_{[f]}^2 \rangle = \frac{\sigma_f^2}{L-1}. \quad (\text{S-23})$$

Therefore, the jackknife estimate for σ_f^2 is given by $(L - 1)s_{[f]}^2$. Interestingly, the error bar $\sqrt{(L - 1)s_{[f]}^2}$ scales as $O(1/\sqrt{L})$, while the the first order correction of the corrected bias is given by $B_\sigma/L - B_\sigma'/(L - 1)$ and is thus of the order of $O(1/L)$. \square

With the framework established, we now proceed with the estimation of $\xi_W^2 = \xi_W^2(\mu_x, \mu_{x^2}, \mu_y)$. Since the data size of each date set, Q_x and Q_y , is $M/2$, Proposition 1 gives us the jackknife estimate of ξ_W^2

$$(M/2)\xi_W^2(\bar{x}, \bar{x^2}, \bar{y}) - (M/2 - 1)\bar{[\xi_W^2]}, \quad \text{where} \quad \bar{[\xi_W^2]} = \frac{1}{M/2} \sum_{i=1}^{M/2} \xi_W^2([x]_i, [x^2]_i, [y]_i) \quad (\text{S-24})$$

and tells us that the bias in this estimate is of order $O(2/M)$. Here, $[x]_i, [x^2]_i, [y]_i$ are jackknife averages

$$[x]_i = \frac{1}{M/2 - 1} \sum_{j \neq i} x_i, \quad [x^2]_i = \frac{1}{M/2 - 1} \sum_{j \neq i} x_i^2, \quad [y]_i = \frac{1}{M/2 - 1} \sum_{j \neq i} y_i. \quad (\text{S-25})$$

Proposition 1 also gives us the uncertainty in the estimation of $\xi_W^2(\mu_x, \mu_{x^2}, \mu_y)$. In particular, it provides the following estimate for the error bar

$$\sqrt{M/2 - 1} \times \sqrt{\bar{[\xi_W^2]}^2 - \left(\bar{\xi_W^2}\right)^2}, \quad \text{where} \quad \bar{[\xi_W^2]}^2 = \frac{1}{M/2} \sum_{i=1}^{M/2} [\xi_W^2([x]_i, [x^2]_i, [y]_i)]^2 \quad (\text{S-26})$$

The estimated error bar scales as $O(1/\sqrt{M/2})$, which is significantly larger than the bias in the estimate of ξ_W^2 . This ensures that the jackknife approach provides a reliable uncertainty quantification while effectively correcting for systematic biases in the estimation process.

C. The complementary simulation results

In the End Matter, we perform Monte Carlo simulations on a specific non-spin-squeezed state to demonstrate that small error bars do not necessarily imply low p-values. Conversely, for spin-squeezed states, the p-value can be used to assess the statistical significance of spin-squeezing generation experiments. To illustrate this, we generate Monte Carlo samples following the previously described state but with $r = 0.985$. This state is characterized by $\xi_W^2 \approx 0.62967$, $\langle 2J_x/N \rangle \approx 0.79600$, and $\text{Var}(2J_x/N) \approx 0.04433$. The corresponding values for $\widehat{\xi_W^2}$ together with the p-value are presented in Fig. S-1 as a function of the number of measurements.

Unlike the non-spin-squeezed scenario discussed in the End Matter, we observe that when the underlying state is spin-squeezed, the p-value upper bound decreases significantly once the number of measurements is high enough. As shown in the figure, without applying this method to assess the confidence of the experimental results, one might incorrectly conclude—due to small error bars—that the state is spin-squeezed with an estimated value of $\xi_W^2 = 0.39815 \pm 0.07112$ from $M = 140$ experimental repetitions (the second simulation result in Figure S-1). However, the computed upper bound on the p-value is $P_{\text{up}} = 0.62904$, indicating that the number of samples is insufficient to support this claim.

This result highlights the necessity of rigorous statistical validation in spin-squeezing experiments. Notably, in our simulation process, no specific probability distribution was assumed, ensuring that the observed misclassification is not a consequence of an improper assumption. The simulation results emphasize that “error bars primarily quantify the spread of the data or the precision of the mean estimate, but do not constitute a rigorous test for statistical significance [6]”. Therefore, to provide a more reliable assessment of spin squeezing, it is essential to incorporate p-values as a complementary statistical measure to properly evaluate the probability that a non-spin squeezed state reproduces the observed statistics.

II. THE OVERLY CONSERVATIVE ESTIMATION FORM THE PARAMETER Γ

As discussed in the main text, we consider the linearized version of the Wineland criterion which is expressed as a function of the variance $\text{Var}(Q_{\vec{n}\perp})$ and the mean $\langle Q_{\vec{n}} \rangle$ as

$$\Gamma = N\text{Var}(Q_{\vec{n}\perp}) - \langle Q_{\vec{n}} \rangle^2. \quad (\text{S-27})$$

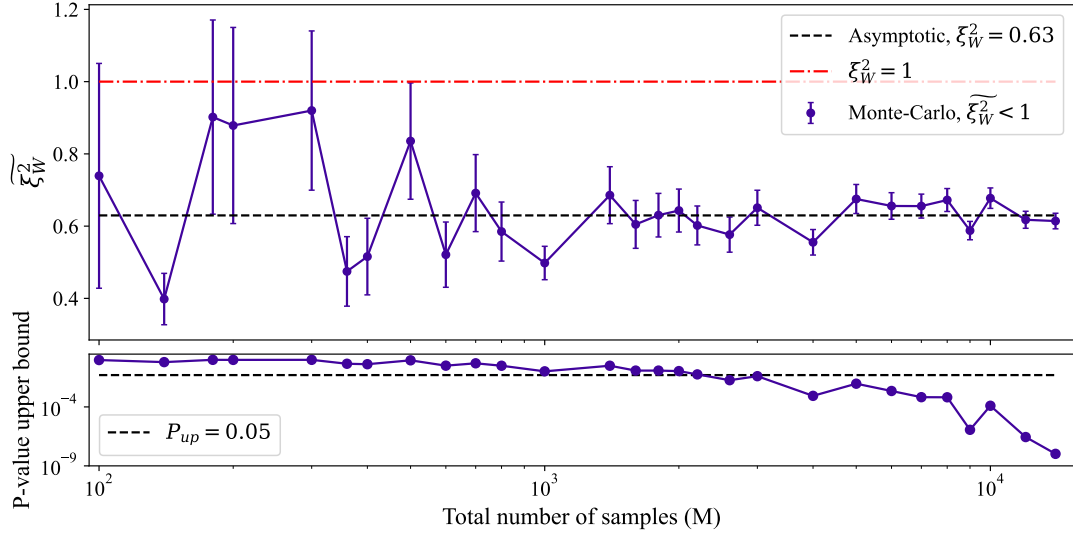


FIG. S-1. (Top) Estimation of the Wineland parameter from Monte Carlo samples of size M sampled from a spin-squeezed state. Two data sets were sampled: one in the eigenbasis of the mean spin direction (J_y) and another in the eigenbasis of the squeezing axis. Each error bar corresponds to one standard deviation. (Bottom) P-value upper bound using the method proposed in the main text on the Monte-Carlo samples.

$Q_{\vec{n}\perp}$ and $Q_{\vec{n}}$ are the normalized angular momentum operators. To estimate the value of Γ experimentally, it is necessary to identify unbiased estimators for $\text{Var}(Q_{\vec{n}\perp})$ and $\langle Q_{\vec{n}} \rangle^2$. The sample variance and sample mean serve as natural choices for these estimators. Specifically, we use for $\text{Var}(Q_{\vec{n}\perp})$ the following sample variance

$$\widetilde{\text{Var}}(Q_{\vec{n}\perp}) = \frac{1}{M_{\vec{n}\perp} - 1} \sum_{k=1}^{M_{\vec{n}\perp}} \left(q_{\vec{n}\perp}^{(k)} - \frac{1}{M_{\vec{n}\perp}} \sum_{j=1}^{M_{\vec{n}\perp}} q_{\vec{n}\perp}^{(j)} \right)^2. \quad (\text{S-28})$$

Here, $M_{\vec{n}\perp}$ is the number of measurements in the direction $\vec{n}\perp$. The term $q_{\vec{n}\perp}^{(k)}$ ($q_{\vec{n}}^{(k)}$) corresponds to the outcome of the measurement operator $2J_{\vec{n}}^{(k)}/N$ ($2J_{\vec{n}\perp}^{(k)}/N$) for experimental round k . For the estimator of $\langle Q_{\vec{n}} \rangle^2$, we use the second moment, which is given by

$$\widetilde{\langle Q_{\vec{n}} \rangle^2} = \frac{1}{M_{\vec{n}}} \sum_{i=1}^{M_{\vec{n}}} q_{\vec{n}}^{(i)2} - \widetilde{\text{Var}}(Q_{\vec{n}}) \quad (\text{S-29})$$

$$= \frac{1}{M_{\vec{n}}} \sum_{k=1}^{M_{\vec{n}}} q_{\vec{n}}^{(k)2} - \frac{1}{M_{\vec{n}} - 1} \sum_{k=1}^{M_{\vec{n}}} \left(q_{\vec{n}}^{(k)} - \frac{1}{M_{\vec{n}}} \sum_{j=1}^{M_{\vec{n}}} q_{\vec{n}}^{(j)} \right)^2. \quad (\text{S-30})$$

It is important to note that both $\widetilde{\langle Q_{\vec{n}} \rangle^2}$ and $\widetilde{\text{Var}}(Q_{\vec{n}\perp})$ are random variables. Using these estimators, the unbiased estimate of the linearized Wineland parameter can be computed as

$$\widetilde{\Gamma} = N \widetilde{\text{Var}}(Q_{\vec{n}\perp}) - \widetilde{\langle Q_{\vec{n}} \rangle^2} = g \left(q_{\vec{n}}^{(1)}, \dots, q_{\vec{n}}^{(M_{\vec{n}})}, q_{\vec{n}\perp}^{(1)}, \dots, q_{\vec{n}\perp}^{(M_{\vec{n}\perp})} \right). \quad (\text{S-31})$$

It is important to note that the function g used in the calculation of $\widetilde{\Gamma}$ cannot be expressed as an estimator of a sum of independent random variables. Instead, g is a nonlinear function of these independent random variables. In this context, McDiarmid's inequality [7, 8] and its various extensions are suited to determine the significance level.

McDiarmid's inequality: McDiarmid's inequality applies to functions that satisfy the bounded differences property, which ensures that small changes in any single input result in only a limited change in the function's output. Specifically, for a function f of independent random variables X_1, X_2, \dots, X_n , the bounded differences property holds if for each i , f changes by at most s_i when substituting the value of the i th coordinate x_i to x'_i , that is

$$\forall i, \sup_{x'_i \in \mathcal{X}_i} |f(x_1, \dots, x_{i-1}, x_i, x_{i+1}, \dots, x_n) - f(x_1, \dots, x_{i-1}, x'_i, x_{i+1}, \dots, x_n)| \leq s_i. \quad (\text{S-32})$$

McDiarmid's inequality then tells us that the deviation of the estimated value of f from its expected value is bounded by

$$\Pr(f(X_1, \dots, X_n) - \mathbb{E}[f(X_1, \dots, X_n)] \geq \epsilon) \leq \exp\left(\frac{-2\epsilon^2}{\sum_{i=1}^n s_i^2}\right). \quad (\text{S-33})$$

However, due to the bounded nature of g and the significant magnitude of the bounded differences s_i which scales as $O(N/M)$, applying McDiarmid's inequality results in a large upper bound on the p-value (see Section V and Fig. S-2). This large bound can lead to an overly conservative estimation when calculating statistical significance, effectively inflating the p-value and making it difficult to achieve strong conclusions regarding the experimental results. In Section V, it is shown that by linearizing Γ , i.e., expressing it as a sum of independent random variables, the negative impact caused by the bounded differences can be effectively avoided.

III. THE UPPER BOUND ON THE P-VALUE FROM THE PARAMETER Γ_c

To calculate the p-value associated to the estimator presented in Eqs. (5) and (6) of the main text, we use Bernstein's inequality [7, 8], which is particularly suited for cases involving independent random variables with known variances.

Bernstein's inequality: Let X_1, X_2, \dots, X_n be independent random variables, each satisfying $|X_i - \mathbb{E}[X_i]| \leq B$. Bernstein's inequality gives an upper bound on the probability that the sum of these variables deviates from its expected value by at least t , that is

$$\Pr\left(\sum_{i=1}^n (X_i - \mathbb{E}[X_i]) \geq t\right) \leq \exp\left(\frac{-t^2}{2(\sum_{i=1}^n \sigma_i^2 + Bt/3)}\right), \quad (\text{S-34})$$

where σ_i^2 is the variance of each variable X_i .

Compared to McDiarmid's inequality, Bernstein's inequality provides a tighter bound because it takes into account the variability of the data through the variance σ_i^2 of each random variable, leading to a more refined estimation of the p-value.

However, in our protocol, we do not make assumptions about the specific quantum states involved. Consequently, we do not have direct access to the true variances σ_i^2 of the underlying variables. To address this challenge, we consider applying the Bathia-Davis inequality [9], which provides an upper bound on the variance from known information about the mean and range of a random variable.

Bathia-Davis inequality: For any random variable X with minimum value a , maximum value b , and mean $\mu = \mathbb{E}[X]$, the variance of X satisfies

$$\text{Var}(X) \leq (b - \mu)(\mu - a). \quad (\text{S-35})$$

By using this inequality, we can estimate an upper bound for the variances of the random variables in our protocol. This allows us to proceed with Bernstein's inequality even without direct knowledge of the variances, ensuring that we still obtain meaningful probabilistic bounds for the p-value in our analysis. To calculate the upper bound of the p-value $P(\tilde{\Gamma}_c \leq \gamma_c | H_0)$, we first state the following proposition.

Proposition 2. *Let Z_1, \dots, Z_l be independent bounded stochastic variables, such that $\mathbb{E}(Z_i) = \mu_z$ and the realization satisfies $a \leq z_i \leq b$, with $a < 0$ and $b > 0$. Also let $Z = \frac{1}{l} \sum_{i=1}^l Z_i$ and $\sigma_z^2 = \frac{1}{l} \sum_{i=1}^l \text{Var}(Z_i)$. Then for the realization $z = \frac{1}{l} \sum_{i=1}^l z_i$ which satisfies $z < 0$ and $\mu_z \geq 0$, one has*

$$P(Z \leq z) \leq \exp\left\{\frac{z^2 l}{2ba - \frac{2}{3}(b-a)z}\right\}. \quad (\text{S-36})$$

Proof. Since $a \leq z_i \leq b$, we have that $|z_i - \mu_z| \leq b - a$. Then from Bernstein's inequality, we obtain the following one-sided inequality

$$P(Z - \mu_z \leq -t) \leq \exp\left\{\frac{-t^2 l}{2\sigma_z^2 + \frac{2}{3}(b-a)t}\right\}, \text{ with } t \geq 0. \quad (\text{S-37})$$

The probability $P(Z \leq z)$, can then be calculated as

$$P(Z \leq z) = P(Z - \mu_z \leq z - \mu_z) \leq \exp \left\{ -\frac{(z - \mu_z)^2 l}{2\sigma_z^2 - \frac{2}{3}(b-a)(z - \mu_z)} \right\}, \quad z < 0 \leq \mu_z. \quad (\text{S-38})$$

By using the Bathias-Davis inequality, we get

$$\sigma_z^2 \leq \max_{i \in [1, \dots, l]} \text{Var}(z_i) \leq (b - \mu_z)(\mu_z - a). \quad (\text{S-39})$$

Combining the above two inequalities, the probability $P(Z \leq z)$ can be bounded by

$$P(Z \leq z) \leq \exp \left\{ \frac{-(z - \mu_z)^2 l}{2(b - \mu_z)(\mu_z - a) - \frac{2}{3}(b - a)(z - \mu_z)} \right\}. \quad (\text{S-40})$$

To analyze the monotonicity of the right-hand side of the above inequality with respect to $\mu_z \geq 0$, we calculate the following derivative

$$\frac{d}{d\mu_z} \frac{-(z - \mu_z)^2}{2(b - \mu_z)(\mu_z - a) - \frac{2}{3}(b - a)(z - \mu_z)} = \frac{3(\mu_z - z)[a(b - \mu_z - 2z) + b(2a - 2\mu_z - z) + 3\mu_z z]}{[a(3b - 2\mu_z - z) + b(z - 4\mu_z) + 3\mu_z^2]^2}. \quad (\text{S-41})$$

Since $(b - \mu_z - 2z) \geq 0$ and $(2a - 2\mu_z - z) \leq 0$, the derivative is less than or equal to 0. Therefore, the right-hand side of the inequality S-40 is monotonic decreasing with μ_z when $\mu_z \geq 0$. The probability $P(Z \leq z)$ can then be further bounded by choosing $\mu_z = 0$ as

$$P(Z \leq z) \leq \exp \left\{ \frac{z^2 l}{2ba + \frac{2}{3}(b-a)z} \right\}. \quad (\text{S-42})$$

□

By using the Proposition 2, we can calculate the upper bound of the p-value $P(\tilde{\Gamma}_c \leq \gamma_c | H_0)$. First, based on the null assumption H_0 , we have $\Gamma \geq 0$. Since $\Gamma_c \geq \Gamma$, it follows that $\Gamma_c \geq 0$, which satisfies the conditions of Proposition 2. Additionally, the values of Γ_c^c given in the main text are always less than 0, and Γ_1^c are always larger than 0, both of which satisfy the conditions for using Proposition 2. Therefore, $P(\tilde{\Gamma}_c \leq \gamma_c | H_0)$ can be upper bounded by

$$P(\tilde{\Gamma}_c \leq \gamma_c | H_0) \leq \exp \left\{ \frac{\gamma_c^2 M/2}{2\Gamma_1^c \Gamma_0^c + 2(\Gamma_1^c - \Gamma_0^c)\gamma_c/3} \right\}. \quad (\text{S-43})$$

Note that this bound does not depend on a specific quantum state, but applies to all states satisfying the condition H_0 . Here, γ_c serves as a variant of the original experimental observation γ and satisfies $\gamma \leq \gamma_c$ for any $c = (\alpha, \beta)$. Note that an important condition is that $\gamma_c < 0$. In experiments, hypothesis testing is conducted only when $\gamma < 0$ is observed. If certain values of $c = (\alpha, \beta)$ result in $\gamma_c \geq 0$, there is a risk of misclassifying a potentially spin-squeezed quantum state as not being spin-squeezed based on criterion Γ_c . Therefore, it is essential to set $\gamma_c < 0$ to prevent such misclassification. This requirement also aligns with the operational criteria outlined in Proposition 2. In the following text, we assume that condition $\gamma_c < 0$ is met by default.

Note that the bound (S-43) is a consequence of $\Gamma_c \geq 0$. Therefore, the same bound also holds when considering the modified null hypothesis H_0^c as “the state of interest satisfies $\Gamma_c \geq 0$ ”, i.e.

$$P(\tilde{\Gamma}_c \leq \gamma_c | H_0^c) \leq \exp \left\{ \frac{\gamma_c^2 M/2}{2\Gamma_1^c \Gamma_0^c + 2(\Gamma_1^c - \Gamma_0^c)\gamma_c/3} \right\}. \quad (\text{S-44})$$

This means that the same p-value applies to both hypotheses.

IV. CONSERVATIVE ASSUMPTIONS FOR THE ESTIMATIONS OF THE NUMBER OF EXPERIMENTAL REPETITIONS

In this section, we explain why the assumptions made during the estimation process are conservative, meaning they result in an underestimation of the number of measurements required to set an upper bound of 5% on the p-value in previously conducted experiments. In our analysis, the criteria for testing spin squeezing is defined as

$$\Gamma_c = N\langle Q_{\vec{n}\perp}^2 \rangle - 2N\alpha\langle Q_{\vec{n}\perp} \rangle - 2\beta\langle Q_{\vec{n}} \rangle + N\alpha^2 + \beta^2. \quad (\text{S-45})$$

Let the sample statistics be $S_{\vec{n}\perp}$, $\mu_{\vec{n}\perp}$ and $\mu_{\vec{n}}$ for the quantities $\text{Var}(Q_{\vec{n}\perp})$, $\langle Q_{\vec{n}\perp} \rangle$ and $\langle Q_{\vec{n}} \rangle$. The estimation of Γ_c can then be deduced from

$$\bar{\gamma}_c = N[S_{\vec{n}\perp} + (\mu_{\vec{n}\perp})^2] - 2N\alpha\mu_{\vec{n}\perp} - 2\beta\mu_{\vec{n}} + N\alpha^2 + \beta^2. \quad (\text{S-46})$$

However, many references on experimental attempts to produce and detect spin squeezing only report the values of the variance $S_{\vec{n}\perp}$ and mean $\mu_{\vec{n}}$, while the information on $\mu_{\vec{n}\perp}$ is either missing or not provided. Hence, we just compute the estimation of Γ_c from

$$\gamma_c = NS_{\vec{n}\perp} - 2\beta\mu_{\vec{n}} + \beta^2. \quad (\text{S-47})$$

In theory, the value of $\mu_{\vec{n}\perp}$ should be zero if the measurements are performed in the ideal directions. However, due to experimental noise and statistical fluctuations, the observed value of $\mu_{\vec{n}\perp}$ may be slightly different from zero. Therefore, we consider all possible values in the range $\mu_{\vec{n}\perp} \in [-0.1, 0.1]$. This represents a significant deviation given that $|\mu_{\vec{n}\perp}| \leq 1$. In practice, if a deviation $|\mu_{\vec{n}\perp}| = 0.1$ is observed, it may indicate that the chosen main direction is not appropriate.

For each dataset, the numerical calculations show that the required number of measurements increases as $|\mu_{\vec{n}\perp}|$ increases. The minimum number of measurements required to achieve a p-value of 0.05 occurs when $\mu_{\vec{n}\perp} = 0$. Conversely, the maximum number of measurements is required when $|\mu_{\vec{n}\perp}| = 0.1$. Therefore, setting $\mu_{\vec{n}\perp} = 0$ offers a conservative estimate of the number of experimental repetitions required to place an upper bound of 5% on the p-value.

The numbers of spins N and experimental repetitions that we have considered are given in the Table I and II below. These tables list the number of measurement repetitions for each experiments [3–5, 10–18] (when not explicitly stated in the paper, we used the maximum number of measurements reported in the article), together with the number of experimental repetitions $M(\mu_{\vec{n}\perp} = 0)$ ($M(\mu_{\vec{n}\perp} = 0.1)$) that would be needed to place an upper bound of 5% on the p-value under the assumption that the mean $\mu_{\vec{n}\perp} = 0$ ($\mu_{\vec{n}\perp} = 0.1$).

TABLE I. The number of Measurements

System size	2[10]	4[11]	9[11]	12[4]	16[11]	21[3]	36[11]	58[3]	64[11]	100[3]	144[5]
Experimental measurements	10000	400	400	1200	400	400	400	400	400	400	2180
$M(\mu_{\vec{n}\perp} = 0.0)$	21200	3260	4160	728	5420	8800	6760	5340	10900	15600	13000
$M(\mu_{\vec{n}\perp} = 0.1)$	23320	3668	4840	842	6420	10460	8080	6400	13040	18800	15600

TABLE II. The number of Measurements

System size	470[5]	1250[12]	1400[13]	33000[14]	50000[15]	90000[16]	480000[17]	740000[18]
Experimental measurements	32500	740	240	200	200	9600	200	2180
$M(\mu_{\vec{n}\perp} = 0.0)$	19970	113800	145800	2204400	1710400	8504400	21070400	118504400
$M(\mu_{\vec{n}\perp} = 0.1)$	24120	137400	176400	2670400	2070400	10270400	25470400	144070400

V. DERIVATION OF OTHER UPPER BOUNDS ASSOCIATED TO Γ

In this section, we compare the upper bounds on the p-value that are obtained using various concentration inequalities. We demonstrate that, in comparison to using the original detection criterion Γ (Eq. 3 of the main text), the family of criteria Γ_c (Eq. 4 of the main text) provides a smaller upper bound on the p-value. This highlights the advantage of our approach in improving the statistical significance of experimental data.

A. The criterion Γ and McDiarmid upper bound

We first continue the analysis started in Section II where we considered the criterion Γ . Specifically, we analyze the property of bounded differences in order to apply McDiarmid's inequality. This property is essential to establish concentration limits on the function g , which depends on independent random variables.

Let the realizations of the random variables $q_n^{(i)}$ and $q_{\vec{n}\perp}^{(j)}$ be x_i and y_j , where $x_i, y_j \in [-1, 1]$, respectively. We thus have

$$\begin{aligned} & \sup_{x_i \in \mathcal{X}_i} \left| g(x_1, \dots, x_k, \dots, x_{M_{\vec{n}}}, y_1, \dots, y_{M_{\vec{n}\perp}}) - g(x_1, \dots, x'_{k'}, \dots, x_{M_{\vec{n}}}, y_1, \dots, y_{M_{\vec{n}\perp}}) \right| \\ &= \sup_{x_i \in \mathcal{X}_i} \frac{N}{M_{\vec{n}} - 1} \left[\frac{2}{M_{\vec{n}}} \sum_{i \neq k} x_i (x'_{k'} - x_k) + \frac{M_{\vec{n}} - 1}{M_{\vec{n}}} (x_k^2 - x'_{k'}^2) \right] \leq \frac{4N}{M_{\vec{n}}} = s_{x,k}, \end{aligned} \quad (\text{S-48})$$

and

$$\begin{aligned} & \sup_{y_i \in \mathcal{Y}_i} \left| g(x_1, \dots, x_{M_{\vec{n}}}, y_1, \dots, y_k, \dots, y_{M_{\vec{n}\perp}}) - g(x_1, \dots, x_{M_{\vec{n}}}, y_1, \dots, y'_{k'}, \dots, y_{M_{\vec{n}\perp}}) \right| \\ &= \sup_{y_i \in \mathcal{Y}_i} \frac{1}{M_{\vec{n}\perp} - 1} \left[\frac{2}{M_{\vec{n}\perp}} \sum_{i \neq k} y_i (y'_{k'} - y_k) + \frac{M_{\vec{n}\perp} - 1}{M_{\vec{n}\perp}} (y_k^2 - y'_{k'}^2) \right] - \frac{1}{M_{\vec{n}\perp}} (y_k^2 - y'_{k'}^2) \leq \frac{4}{M_{\vec{n}\perp}} = s_{y,k}. \end{aligned} \quad (\text{S-49})$$

With the bounded difference $\{s_{x,k}, s_{y,k}\}$, the significance level $P(\Gamma \leq \gamma | H_0)$ can be bounded by

$$P(\tilde{\Gamma} \leq \gamma | H_0) = P(\tilde{\Gamma} - \Gamma \leq \gamma - \Gamma | H_0) \leq \exp \left\{ \frac{-2(\gamma - \Gamma)^2}{\frac{16N^2}{M_{\vec{n}}} + \frac{16}{M_{\vec{n}\perp}}} \right\} \leq \exp \left\{ \frac{-\gamma^2}{\frac{8N^2}{M_{\vec{n}}} + \frac{8}{M_{\vec{n}\perp}}} \right\}. \quad (\text{S-50})$$

The denominator in the above expression contains an N^2 term, which causes the p-value to increase rapidly as N grows. This leads to a large upper bound on the p-value, necessitating more measurements to counterbalance the N^2 effect. The solution we propose in the main text is to focus on the family of criteria Γ_c , which is expressed as a sum of independent random variables and avoids the N^2 term introduced by the bounded differences. Below, we introduce an other approach based on Bernstein's inequality to deal with the N^2 problem.

B. Bernstein's bound with Γ

We assume that 4 identical and independent experiments are performed, with half of them reporting on the measurement result of the angular momentum operator in the direction \vec{n} while the rest is in the orthogonal direction $\vec{n}\perp$. Then, from the collected data $\{q_{\vec{n}}^{(1)}, q_{\vec{n}}^{(2)}, q_{\vec{n}\perp}^{(1)}, q_{\vec{n}\perp}^{(2)}\}$, we estimate the variance using sample variance and the second moment by sample mean square. We get

$$\widetilde{\Gamma}'_1 = \frac{N}{2} \left(q_{\vec{n}\perp}^{(1)} - q_{\vec{n}\perp}^{(2)} \right)^2 - q_{\vec{n}}^{(1)} q_{\vec{n}}^{(2)}. \quad (\text{S-51})$$

This process is repeated $L = M/4$ times with M the number of experimental realizations, such that the estimator of Γ turns into the sum of random independent variables,

$$\widetilde{\Gamma}' = \frac{1}{L} \sum_{i=1}^L \widetilde{\Gamma}'_i, \quad (\text{S-52})$$

with

$$\widetilde{\Gamma}'_i = \frac{N}{2} \left(q_{\vec{n}\perp}^{(2i-1)} - q_{\vec{n}\perp}^{(2i)} \right)^2 - q_{\vec{n}}^{(2i-1)} q_{\vec{n}}^{(2i)}. \quad (\text{S-53})$$

It is easy to find that the estimator (S-52) is unbiased:

$$\mathbb{E}(\widetilde{\Gamma}') = \Gamma. \quad (\text{S-54})$$

Notice that the maximum and minimum values of (S-53) are $2N + 1$ and -1 , respectively. From the Proposition 2, we find

$$P(\tilde{\Gamma}' \leq \gamma | H_0) \leq \exp \left\{ -\frac{\gamma^2 M/8}{2N + 1 - 2\gamma(N + 1)/3} \right\}. \quad (\text{S-55})$$

From the previous result, the number of independent experimental realizations required to set an upper bound p on the p-value is

$$M = 16 \frac{\log 1/p}{\gamma^2} \left[(N + 1) \left(1 - \frac{\gamma}{3} \right) - \frac{1}{2} \right]. \quad (\text{S-56})$$

In Fig. S-2, we show the number of experiments based on different concentration inequalities. The method introduced in the main text and detailed in Section III, which relies on the linearized parameter Γ_c together with Bernstein's bound, is the one that systematically requires the fewest number of measurements. On the other hand, the approach based on the parameter Γ together with McDiarmid's inequality requires the most measurements, as it employs the bounded differences property, which demands a large number of measurements to offset the N^2 effect. The Bernstein's inequality to the parameter Γ using the technique where four independent measurements are considered in each round of the experiment is also shown. This allows Γ to be expressed as a sum of independent random variables, and as a result, the p-value only contains the term N , without the N^2 component. Therefore, compared to the method based on McDiarmid's inequality, the number of required measurements is reduced. This highlights the importance of a well-designed linear estimator, which can significantly reduce the required number of experimental measurements.

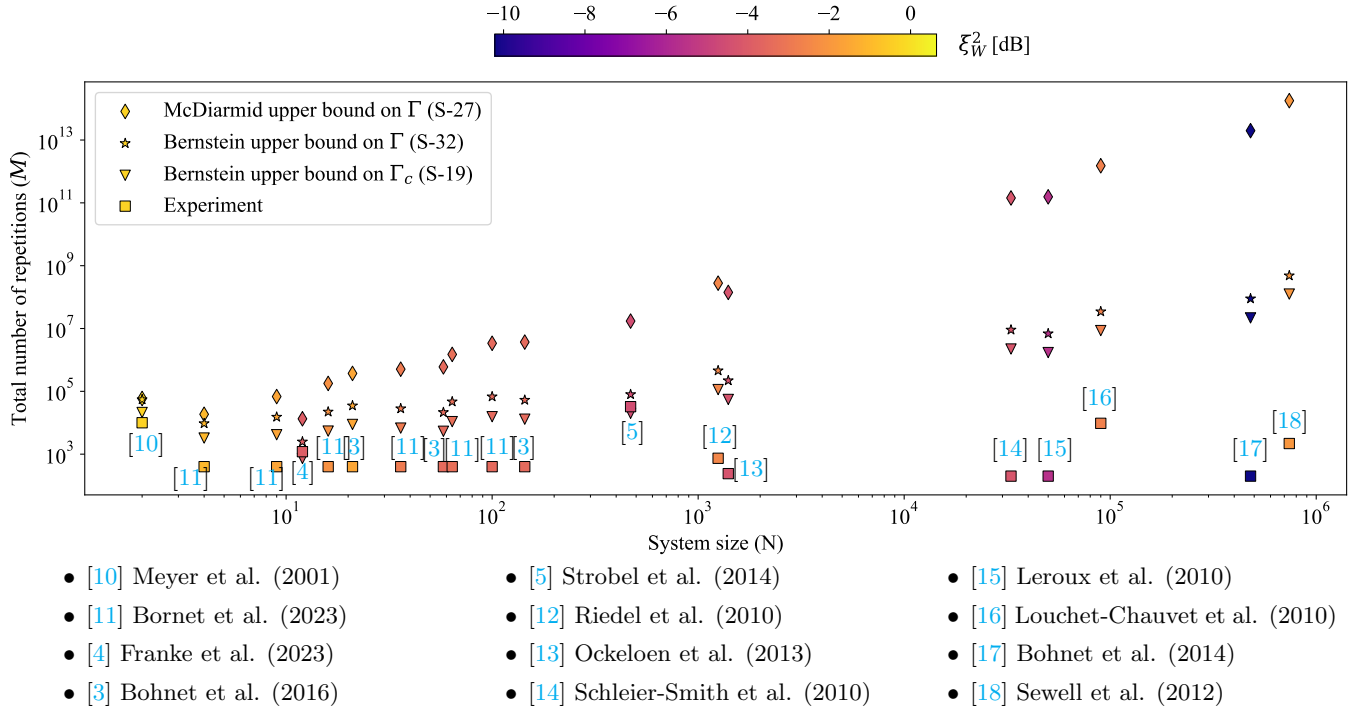


FIG. S-2. **Comparison of the number of experimental realizations based on different concentration inequalities.** The experiments reported in the literature are represented by squares, where the position indicates the total number of experimental repetitions (M) and the system size (N) that were realized. When calculating the number of measurements required to achieve a p-value of 0.05 using McDiarmid's inequality (marked by diamonds), we assumed equal number of measurements in both measurement directions. The stars represent the Bernstein upper bound applied to Γ , calculated using S-32. The downward triangles correspond to the Bernstein upper bound, applied to the linearized parameter Γ_c , as reported presented in the main text.

VI. DERIVATION OF THE LOWER BOUND ON THE P-VALUE

In this section, we focus on the lower bound of the p-value. We start with the mixed state

$$\hat{\rho} = r |\chi\rangle\langle\chi| + \frac{1-r}{2} (|\uparrow_{\vec{n}_\perp}\rangle\langle\uparrow_{\vec{n}_\perp}| + |\downarrow_{\vec{n}_\perp}\rangle\langle\downarrow_{\vec{n}_\perp}|). \quad (\text{S-57})$$

Here $|\chi\rangle$ is a spin squeezed state with mean spin direction given by \vec{n} . We also have $|\uparrow_{\vec{n}_\perp}\rangle = |\uparrow_{\vec{n}_\perp}\rangle^{\otimes N}$, $|\downarrow_{\vec{n}_\perp}\rangle = |\downarrow_{\vec{n}_\perp}\rangle^{\otimes N}$ and $0 \leq r \leq 1$. We have

$$\langle Q_{\vec{n}} \rangle = \text{Tr}[Q_{\vec{n}} \hat{\rho}] = r \langle Q_{\vec{n}} \rangle_{|\chi\rangle}, \quad (\text{S-58})$$

$$\langle Q_{\vec{n}_\perp} \rangle = \text{Tr}[Q_{\vec{n}_\perp} \hat{\rho}] = 0. \quad (\text{S-59})$$

Since

$$Q_{\vec{n}_\perp} = \frac{1}{N} \sum_i^N \sigma_{\vec{n}_\perp}^{(i)}, \quad (\text{S-60})$$

we have

$$\langle \uparrow_{\vec{n}_\perp} | (Q_{\vec{n}_\perp})^2 | \uparrow_{\vec{n}_\perp} \rangle = \langle \downarrow_{\vec{n}_\perp} | (Q_{\vec{n}_\perp})^2 | \downarrow_{\vec{n}_\perp} \rangle = \frac{1}{N^2} (N + N^2 - N) = 1 \quad (\text{S-61})$$

and

$$\text{Var}(Q_{\vec{n}_\perp}) = r \langle Q_{\vec{n}_\perp}^2 \rangle_{|\chi\rangle} + 1 - r. \quad (\text{S-62})$$

With the above results, the Wineland parameter is given by

$$\xi_W^2 = \frac{rN \langle Q_{\vec{n}_\perp}^2 \rangle_{|\chi\rangle} + (1-r)N}{r^2 \langle Q_{\vec{n}} \rangle_{|\chi\rangle}^2} = \frac{1}{r} \xi_W^2 (|\chi\rangle) + \frac{1-r}{r^2} \frac{N}{\langle Q_{\vec{n}} \rangle_{|\chi\rangle}^2}. \quad (\text{S-63})$$

Under the assumption that $\hat{\rho}$ is not a spin-squeezed state, ξ_W^2 should be equal to or larger than 1. Therefore, the parameter r for such a state satisfies

$$r^2 + \left(\frac{N}{\langle Q_{\vec{n}} \rangle_{|\chi\rangle}^2} - \xi_W^2 (|\chi\rangle) \right) r - \frac{N}{\langle Q_{\vec{n}} \rangle_{|\chi\rangle}^2} \leq 0, \quad (\text{S-64})$$

which gives

$$r \leq r_{\max} = \frac{1}{2} \left(\kappa + \sqrt{\kappa^2 + \frac{4N}{\langle Q_{\vec{n}} \rangle_{|\chi\rangle}^2}} \right) \quad (\text{S-65})$$

where $\kappa = \xi_W^2 (|\chi\rangle) - N/\langle Q_{\vec{n}} \rangle_{|\chi\rangle}^2$. Note that r_{\max} can be lower bounded by

$$r_{\max} \geq \min_{\kappa, \langle Q_{\vec{n}} \rangle_{|\chi\rangle}^2} r_{\max} = \frac{\sqrt{N^2 + 4N} - N}{2}, \quad (\text{S-66})$$

achieved for $\xi_W^2 = 0$ and $\langle Q_{\vec{n}} \rangle_{|\chi\rangle}^2 = 1$.

It should also be noted that the state $\hat{\rho}$ may not be the best state to construct the lower bound, i.e. there could exist other quantum states that bring the lower bound of the p-value closer to the upper bound. Further exploration of alternative states could lead to a more accurate and tighter bound on the p-value.

[1] P. Guilmin, R. Gautier, A. Bocquet, É. Genois, and D. Weiss, *Dynamiqs: an open-source python library for gpu-accelerated and differentiable simulation of quantum systems* (2024).

- [2] F. Becca and S. Sorella, *Quantum Monte Carlo approaches for correlated systems* (Cambridge University Press, 2017).
- [3] J. G. Bohnet, B. C. Sawyer, J. W. Britton, M. L. Wall, A. M. Rey, M. Foss-Feig, and J. J. Bollinger, Quantum spin dynamics and entanglement generation with hundreds of trapped ions, *Science* **352**, 1297–1301 (2016).
- [4] J. Franke, S. R. Muleady, R. Kaubruegger, F. Kranzl, R. Blatt, A. M. Rey, M. K. Joshi, and C. F. Roos, Quantum-enhanced sensing on optical transitions through finite-range interactions, *Nature* **621**, 740–745 (2023).
- [5] H. Strobel, W. Muessel, D. Linnemann, T. Zibold, D. B. Hume, L. Pezzè, A. Smerzi, and M. K. Oberthaler, Fisher information and entanglement of non-gaussian spin states, *Science* **345**, 424–427 (2014).
- [6] M. Krzywinski and N. Altman, Error bars, *Nature Methods* **10**, 921 (2013).
- [7] C. McDiarmid, On the method of bounded differences, in *Surveys in Combinatorics, 1989* (Cambridge University Press, 1989) p. 148–188.
- [8] C. McDiarmid, Concentration, in *Probabilistic Methods for Discrete Math.*, edited by M. Habib, C. McDiarmid, J. Ramirez-Alfonsin, and B. Reed (Springer Berlin Heidelberg, Berlin, Heidelberg, 1998) pp. 195–248.
- [9] R. Bhatia and C. Davis, A better bound on the variance, *The American Mathematical Monthly* **107**, 353–357 (2000).
- [10] V. Meyer, M. A. Rowe, D. Kielpinski, C. A. Sackett, W. M. Itano, C. Monroe, and D. J. Wineland, Experimental demonstration of entanglement-enhanced rotation angle estimation using trapped ions, *Phys. Rev. Lett.* **86**, 5870 (2001).
- [11] G. Bornet, G. Emperaiger, C. Chen, B. Ye, M. Block, M. Bintz, J. A. Boyd, D. Barredo, T. Comparin, F. Mezzacapo, T. Roscilde, T. Lahaye, N. Y. Yao, and A. Browaeys, Scalable spin squeezing in a dipolar rydberg atom array, *Nature* **621**, 728–733 (2023).
- [12] M. F. Riedel, P. Böhi, Y. Li, T. W. Hänsch, A. Sinatra, and P. Treutlein, Atom-chip-based generation of entanglement for quantum metrology, *Nature* **464**, 1170–1173 (2010).
- [13] C. F. Ockeloen, R. Schmied, M. F. Riedel, and P. Treutlein, Quantum metrology with a scanning probe atom interferometer, *Phys. Rev. Lett.* **111**, 143001 (2013).
- [14] M. H. Schleier-Smith, I. D. Leroux, and V. Vuletić, States of an ensemble of two-level atoms with reduced quantum uncertainty, *Phys. Rev. Lett.* **104**, 073604 (2010).
- [15] I. D. Leroux, M. H. Schleier-Smith, and V. Vuletić, Implementation of cavity squeezing of a collective atomic spin, *Phys. Rev. Lett.* **104**, 073602 (2010).
- [16] A. Louchet-Chauvet, J. Appel, J. J. Renema, D. Oblak, N. Kjaergaard, and E. S. Polzik, Entanglement-assisted atomic clock beyond the projection noise limit, *New J. Phys.* **12**, 065032 (2010).
- [17] J. G. Bohnet, K. C. Cox, M. A. Norcia, J. M. Weiner, Z. Chen, and J. K. Thompson, Reduced spin measurement back-action for a phase sensitivity ten times beyond the standard quantum limit, *Nat. Photon.* **8**, 731–736 (2014).
- [18] R. J. Sewell, M. Koschorreck, M. Napolitano, B. Dubost, N. Behbood, and M. W. Mitchell, Magnetic sensitivity beyond the projection noise limit by spin squeezing, *Phys. Rev. Lett.* **109**, 253605 (2012).